Search for heavy resonances decaying to a photon and a hadronically decaying $Z/W/H$ boson in pp collisions at $\sqrt{s} = 13$ TeV with the ATLAS detector

M. Aaboud *et al.*[*]
(ATLAS Collaboration)

(Received 8 May 2018; published 28 August 2018)

Many extensions of the Standard Model predict new resonances decaying to a Z, W, or Higgs boson and a photon. This paper presents a search for such resonances produced in pp collisions at $\sqrt{s} = 13$ TeV using a data set with an integrated luminosity of 36.1 fb^{-1} collected by the ATLAS detector at the LHC. The $Z/W/H$ bosons are identified through their decays to hadrons. The data are found to be consistent with the Standard Model expectation in the entire investigated mass range. Upper limits are set on the production cross section times branching fraction for resonance decays to $Z/W + \gamma$ in the mass range from 1.0 to 6.8 TeV and for the first time into $H + \gamma$ in the mass range from 1.0 to 3.0 TeV.

DOI: 10.1103/PhysRevD.98.032015

I. INTRODUCTION

Many proposals for physics beyond the Standard Model (SM) include the prediction of new massive bosons. Examples are Technicolor [1] or little Higgs [2], as well as extensions to the SM Higgs sector such as including an additional electroweak singlet scalar [3]. Decay modes of these new bosons include final states with a Z or a W boson and a photon. In addition, decays of heavy spin-1 bosons to the 125 GeV Higgs boson and a photon present an interesting search channel [4]. This paper describes a search for massive neutral and charged bosons decaying to a photon and a Z, W, or Higgs boson with subsequent hadronic decay of these bosons. The search uses 36.1 fb^{-1} of proton-proton (pp) collision data at a center-of-mass energy $\sqrt{s} = 13$ TeV collected with the ATLAS detector in 2015 and 2016.

The selection of events collected for this search is based on the presence of high transverse energy photons. The identification of Z, W, and Higgs bosons exploits properties of the highly boosted bosons with merged dijet energy clusters reconstructed as a large-radius jet. The advantage of this final state is that a large fraction of events from the heavy resonance decay is detected since the branching fraction of Z and W bosons into hadrons is approximately 70%. The Higgs boson also decays mainly hadronically, dominated by the decay to a $b\bar{b}$ quark pair with a branching fraction of 58%. The measurements use the mass of the large-radius jet and other substructure information to identify the Z, W, and Higgs bosons. In addition, for the Z and Higgs bosons, the sensitivity is increased by identifying the long-lived decays of bottom hadrons within jets.

Previous searches for high-mass resonances decaying to a Z boson and a photon were conducted by the Tevatron's D0 experiment [5] as well as at the LHC. The ATLAS experiment performed searches for heavy resonances decaying to a Z or a W boson and a photon, with subsequent leptonic decays of the Z and W bosons, using data collected at $\sqrt{s} = 7$ and 8 TeV [6,7], and for heavy resonances decaying to a Z boson and a photon using 3.2 fb^{-1} of $\sqrt{s} = 13$ TeV data [8]. In the latter search, both the leptonic and hadronic decays of the Z boson were used. The ATLAS experiment also used a 36.1 fb^{-1} data set collected at $\sqrt{s} = 13$ TeV to search for resonances decaying to a Z boson and a photon with the decays $Z \to e^+e^-, \mu^+\mu^-$ [9] and $\nu\bar{\nu}$ [10]. The CMS experiment performed searches for a heavy resonance decaying to a photon and a hadronically or leptonically decaying Z boson using data sets collected at $\sqrt{s} = 7$, 8, and 13 TeV [11–14]. None of the searches revealed the presence of a new resonance.

In the present search, scans of invariant mass spectra of the photon–jet system between 1.0 and 6.8 TeV are used to search for narrow signal resonances, denoted generically by X hereafter, decaying to a Z, W, or Higgs boson and a photon. A variety of production and decay models is considered in order for the search to be sensitive to Higgs-like (spin-0), W-like (spin-1), and graviton-like (spin-2) bosons [15,16]. Gluon–gluon fusion production is considered for spin-0 and spin-2 resonances decaying to $Z\gamma$ [15]. Production via quark-antiquark annihilation is

[*]Full author list given at the end of the article.

considered for a spin-2 resonance decaying to $Z\gamma$ [15], a spin-1 resonance decaying to $W\gamma$ [16], and for the first time a spin-1 $H\gamma$ resonance.

II. ATLAS DETECTOR

The ATLAS detector [17] consists of a tracking detector within a superconducting solenoid providing a 2 T axial magnetic field, electromagnetic and hadronic calorimeters, and a muon spectrometer incorporating three large superconducting toroid magnets. The inner detector, consisting of silicon pixel, silicon microstrip, and transition radiation tracking detectors, covers the pseudorapidity[1] range $|\eta| < 2.5$. The energies of photons and jets are measured primarily by the calorimeter system, which covers the pseudorapidity range $|\eta| < 4.9$. The electromagnetic calorimeter is a high-granularity liquid-argon (LAr) sampling calorimeter with lead absorber plates and is located just outside the solenoid. It spans the region $|\eta| < 3.2$ with barrel and end cap sections, segmented into three layers longitudinal in shower–depth in the region $|\eta| < 2.5$, with $\Delta\eta \times \Delta\phi$ readout granularity in the second layer of 0.025×0.025. Beyond the cryostat of the electromagnetic calorimeter, a steel/scintillator tile hadronic calorimeter covers the region $|\eta| < 1.7$. It is also segmented into three layers longitudinal in shower depth with a lateral readout granularity of 0.1×0.1 in $\Delta\eta \times \Delta\phi$. Two copper/LAr hadronic end cap calorimeters with similar granularity cover the region $1.5 < |\eta| < 3.2$. In the forward region, electromagnetic and hadronic energy measurements are provided by copper/LAr and tungsten/LAr modules, respectively. A two-level trigger system [18] is used to select the events to be recorded. The first level of the trigger is implemented in hardware using a subset of the detector information to reduce the event rate to at most 100 kHz from the beam bunch crossing rate of 40 MHz. The final data selection is done with a software-based trigger that reduces the event rate to an average of 1 kHz.

III. DATA AND MONTE CARLO SAMPLES

The data used in this search were collected in 2015 and 2016 from LHC pp collisions with a 13 TeV center-of-mass energy and 25 ns bunch spacing. In these collisions, the average number of inelastic pp collisions in each bunch crossing (referred to as pileup) was approximately 25. Events were recorded using a single-photon trigger that imposed a transverse energy threshold of 140 GeV and loose photon identification requirements based on cluster shower-shape variables [19]. The photon trigger is fully efficient for the events selected for this analysis. After requiring all ATLAS subdetectors to be operational, the resulting integrated luminosity is 36.1 fb^{-1}.

Simulated signal events are used to optimize the event identification and estimate the efficiency of the event reconstruction and selection. SM background processes were simulated to test the parametrization of the jet–photon invariant mass spectra, which is used in the data-driven estimation of the background. All simulated signal and background event samples were generated with Monte Carlo (MC) techniques as described below.

The production and decay of spin-0 and spin-2 $Z\gamma$ resonances, spin-1 $W\gamma$ resonances, and spin-1 $H\gamma$ resonances were modeled assuming a narrow-width approximation. The decay width of each resonance was set to 4 MeV, which is much smaller than the experimental resolution, and interference between these resonant processes and nonresonant SM production of the corresponding final states was neglected.

The $Z\gamma$ scalar resonances produced via gluon–gluon fusion, $gg \to X \to Z\gamma$, were modeled by POWHEG-BOX [20,21], with the CT10 parton distribution function (PDF) set [22], interfaced with PYTHIA8.186 [23] for the underlying event, parton showering, and hadronization with the CTEQ6L1 PDF set [24] and a set of tuned underlying-event parameters called the AZNLO tune [25]. This model is the same as that used for SM $H \to Z\gamma$ production with the resonance mass varied but the width held fixed.

The spin-2 $gg \to X \to Z\gamma$ and $q\bar{q} \to X \to Z\gamma$ and the spin-1 $q\bar{q} \to X \to W\gamma$ and $q\bar{q} \to X \to H\gamma$ resonant processes were modeled via effective couplings implemented in MADGRAPH5_AMC@NLOV2.3.3 [26], interfaced to the PYTHIA8.186 parton shower model with the A14 parameter tune [27] and the NNPDF2.3LO PDF set [28]. The $Z\gamma$ models produce transversely polarized Z bosons, and the $W\gamma$ models produce longitudinally polarized W bosons. In these samples, the W and Z bosons are forced to decay hadronically, and the Higgs boson is forced to decay to $b\bar{b}$.

The dominant SM backgrounds are prompt photons produced in association with jets, hadronically decaying W or Z bosons produced in association with a photon, and $t\bar{t} + \gamma$ events. The samples of events containing a photon with associated jets were simulated using the SHERPA2.1.1 generator [29], requiring a photon transverse energy above 35 GeV. Matrix elements were calculated at leading order with up to either three or four partons, depending on the transverse energy of photon. They were then merged with the SHERPA parton shower [30] using the ME+PS@LO prescription [31]. SHERPA2.1.1 was also used to simulate events containing an on-shell, hadronically decaying W or Z boson and a photon. Matrix elements were calculated with up to three additional partons at leading order using the COMIX [32] and OPENLOOPS [33] matrix element generators and merged with the SHERPA parton shower

[1]ATLAS uses a right-handed coordinate system with its origin at the nominal interaction point (IP) in the center of the detector and the z axis along the beam pipe. The x axis points from the IP to the center of the LHC ring, and the y axis points upward. Cylindrical coordinates (r, ϕ) are used in the transverse plane, ϕ being the azimuthal angle around the z axis. The pseudorapidity is defined in terms of the polar angle θ as $\eta = -\ln\tan(\theta/2)$.

using the ME+PS@NLO prescription [34]. For these $\gamma +$ jet and $W/Z + \gamma$ simulations, the CT10 PDF set was used in conjunction with a dedicated parton shower tuning developed by the authors of SHERPA. The $t\bar{t} + \gamma$ events were modeled using MADGRAPH5_AMC@NLOV2.3.3 interfaced to the PYTHIA8.186 parton shower with the A14 parameter tune and the NNPDF2.3LO PDF set. In all MC samples, EVTGEN1.2.0 [35] was used to model charm and beauty hadron decays.

The simulated signal and SM background events were processed by a detailed GEANT4 [36] simulation of the ATLAS detector [37]. In all simulated signal and background samples, the effects of overlapping inelastic pp collisions were included by overlaying multiple events simulated with PYTHIA8.186 using the A3 set of tuned parameters [38] and the MSTW2008LO PDF set [39]. The simulated events were weighted so that the distribution of the number of pileup interactions in the simulation matched the one in the data. The simulated events were then passed through the same event reconstruction algorithms used for the data, including corrections for known differences between data and simulation in the efficiencies of photon reconstruction and selection, in the photon and jet energy scale and resolution, and in the tagging efficiency of heavy-flavor jets.

IV. EVENT SELECTION

A. Reconstruction of photons and jets

The photon reconstruction is described in Ref. [40]. A discriminant, based on lateral and longitudinal shower profiles, is constructed to distinguish prompt photons from hadrons as well as photons from decays of mesons inside jets. In this analysis, two levels of selections are applied: the *loose* selection criterion defined in Ref. [40] at the trigger level and the *tight* selection criterion for the final analysis selection. In the final selection, photon candidates are required to have transverse energy above 250 GeV and pseudorapidity $|\eta| < 1.37$. These criteria are applied to reduce the contribution from the SM production of prompt photons with associated jets. The efficiency of a photon within that region to pass the tight selection criterion is above 90%. The transverse energy $E_{\mathrm{T,iso}}$, deposited within a cone of size $\Delta R \equiv \sqrt{(\Delta\eta)^2 + (\Delta\phi)^2} = 0.4$ around the photon cluster, is corrected for the photon energy deposited outside of the cluster, underlying event, and multiple pp interactions; it is required to satisfy $E_{\mathrm{T,iso}} < 2.45\ \mathrm{GeV} + 0.022\ E_{\mathrm{T}}^{\gamma}$, where E_{T}^{γ} is the transverse energy of the photon cluster. The requirement is applied to reduce contamination from hadrons misidentified as photons and is 98% efficient for prompt photons passing the tight criterion. Corrections mitigating the differences between the calorimeter response to photons in data and simulation are derived using collision data. The photon energy calibration is derived using samples of simulated events followed by data-driven corrections [41].

Large-radius (large-R) jets are reconstructed from topological energy clusters (topocluster) [42] in the calorimeter, using the anti-k_t algorithm [43] with a radius parameter $R = 1.0$. To reduce contributions to the jet transverse momentum (p_{T}) and mass arising from pileup, a trimming procedure [44] is applied in which subjets with $R = 0.2$ and carrying less than 5% of the original p_{T} of the jet are removed. Jets are calibrated to the level of stable final-state particles using simulation [45]. Differences between data and simulation in the jet energy scale and resolution are corrected using *in situ* methods [46]. The jet energy resolution for jets with p_{T} of 1 TeV is approximately 5%. Jet candidates are required to have p_{T} above 200 GeV and $|\eta| < 2.0$ to ensure tracking detector coverage within the jet cone. The jet candidates are required to be separated from any photon candidate by $\Delta R > 1.0$.

The jet mass is computed as a weighted combination of *calorimetric mass* and *track-assisted mass* [47]. The calorimetric mass is computed from the massless topocluster four-momenta. The track-assisted mass incorporates information from the calorimeter and the four-momenta of tracks, which are matched to the jets using ghost association [48] and are matched to the primary vertex, which is defined as the vertex with largest sum of squared momenta of associated tracks in the event [49]. The relative weighting of the calorimetric and track-assisted mass in the final mass calculation is based on the expected resolutions of the two mass variables. The mass resolution in the peak of the jet mass distribution for jets originating from Z, W, or Higgs bosons ranges from 7% to 15% for jets with transverse momenta of 500 to 2500 GeV. Reconstructed jet mass distributions for various signal hypotheses are shown in Fig. 1. Peaks centered at the Z, W, and Higgs boson masses are clearly visible. In the mass distributions of jets arising from the Z and Higgs boson decays, a feature at low jet invariant mass is also prominent for decays of resonances with masses of 2 TeV or lower. This is a result of energy flow outside of the jet cone. For the $W\gamma$ spin-1 resonance decays, the effect is mitigated due to the longitudinal polarization of the W boson, which enhances the collimation of the decay products. The lower-mass side of the cores of the Z boson and Higgs boson mass peaks are enhanced from loss of neutrino energy in the jet when at least one of the b-hadrons decays semileptonically.

The jet mass and the $D_2^{(\beta=1)}$ jet substructure discriminant are employed to distinguish between jets originating from hadronically decaying Z or W bosons and jets originating from quarks and gluons. The variable $D_2^{(\beta=1)}$ is defined as the ratio of two-point and three-point energy correlation functions [50,51], which are based on the energies and pairwise angular distances of particles within a jet. The performance of this discriminant has been studied in MC simulations and data [52,53]. Upper and lower bounds on

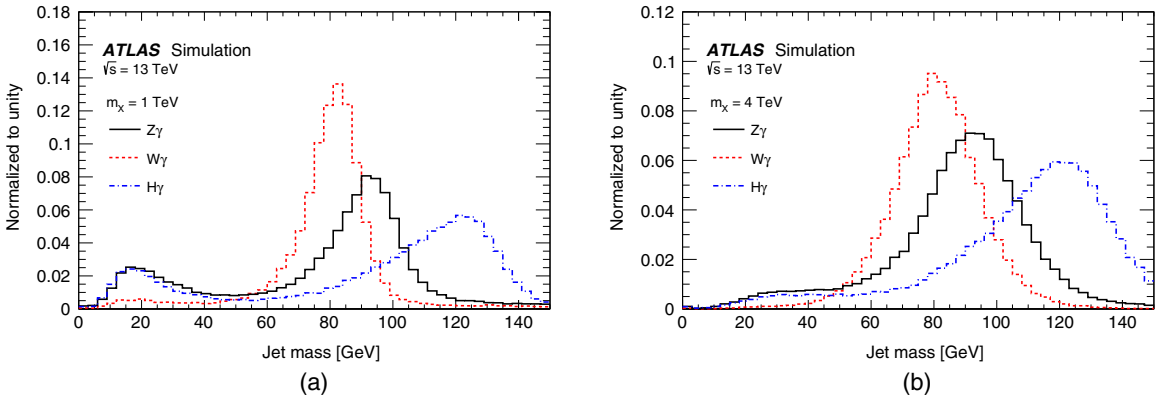

FIG. 1. The mass distributions of large-R jets originating from Z, W, and H bosons resulting from decays of a resonance with a mass (a) $m_X = 1$ TeV and (b) $m_X = 4$ TeV in samples of simulated events. Only the hadronic Z, W, and $H \to b\bar{b}$ decays are considered in these figures. Only the spin-0 model is shown for the $Z\gamma$ decay as the jet mass distribution is not sensitive to the signal spin hypothesis.

the jet mass and upper bound on $D_2^{(\beta=1)}$ are tuned to achieve 50% efficiency for jets with p_{T} in the range of 300 to 2500 GeV from decays of a Z or W boson. The fraction of jets originating from a quark or a gluon passing this selection varies between approximately 2.2% and 1.3% in this p_{T} range. The $D_2^{(\beta=1)}$ discriminant is not used for the $H \to b\bar{b}$ selection.

Track jets are reconstructed using the anti-k_t algorithm with radius parameter $R = 0.2$ and tracks matched to the large-R jets using ghost association. Track jets that contain b-hadrons are identified using the MV2C10 tagging algorithm, which exploits the lifetime of b-hadrons and the kinematic properties of their charged decay products [54,55]. The efficiency of the algorithm is 70% when applied to b jets in simulated $t\bar{t}$ events. The fraction of track jets originating from a light quark or a gluon, tagged as originating from a b-hadron, is approximately 0.8% in simulated $t\bar{t}$ events.

B. Event selection and categorization

Events considered for analysis are triggered by the presence of a photon candidate with p_{T} greater than 140 GeV. A small fraction of events in which adverse instrumental effects were identified is removed. The baseline selection identifies events with one photon candidate and one large-R jet candidate. If more than one photon or jet candidate is found, only the highest-p_{T} objects are considered further. The efficiency of the selection for a resonance with a mass of 3 TeV varies from approximately 60% to 80% depending on the signal hypothesis, as shown in Fig. 2. The decrease of the baseline selection efficiency for resonances with lower mass is due to the kinematic thresholds of 200 and 250 GeV required for the jet and photon p_{T} respectively. Differences in the baseline efficiencies between the resonance types are due to different angular distributions of the produced photon-jet system (depending on the spin hypothesis and production mode) and therefore different probabilities to pass the photon and jet p_{T} and $|\eta|$ requirements.

Following the baseline selection, events are classified into four or fewer subsamples to improve the expected signal sensitivity. The categorization is made in order of decreasing background rejection to achieve high sensitivity throughout the resonance mass (m_X) range. For resonance masses below 3 TeV, it is desirable to maximally suppress the SM background, while for very high m_X values, due to the steeply falling jet-photon invariant mass ($m_{\mathrm{J}\gamma}$) distribution of background processes, a loose selection is appropriate. For the $Z\gamma$ search, the categories, defined in the next paragraph, are BTAG, D2, VMASS, and ELSE. In the $W\gamma$ search, only the D2,

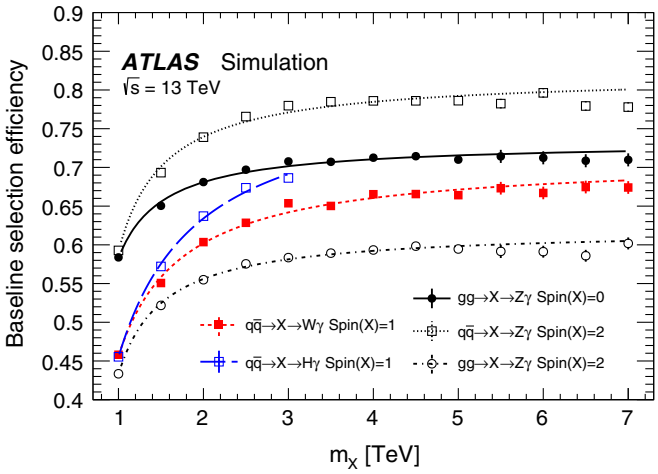

FIG. 2. Efficiencies for signal events to pass the baseline selection as a function of the resonance mass m_X for different signal models, production modes, and spin hypotheses. The uncertainty bars shown are statistical only. The lines represent polynomial fits to the simulated data points. The line corresponding to the $H\gamma$ resonance baseline selection efficiency is discontinued above m_X of 3 TeV since the search for $H\gamma$ does not cover this resonance mass region.

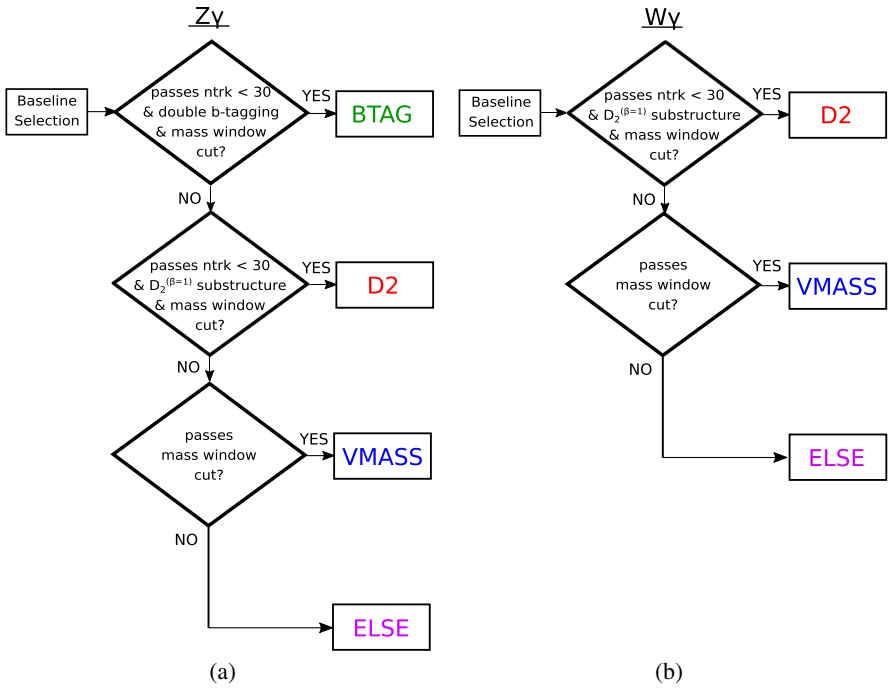

FIG. 3. Flow charts of the categorization of the events in (a) $Z\gamma$ and (b) $W\gamma$ searches. In the $H\gamma$ search, only the BTAG selection is applied, analogous to that applied in the $Z\gamma$ search.

VMASS, and ELSE categories are used. The $H\gamma$ search employs only the BTAG category. The process of event categorization proceeds sequentially starting from the events found in the baseline selection as shown in the diagrams in Fig. 3.

The first subsample in the $Z\gamma$ and $H\gamma$ searches, the BTAG category, captures events in which the two leading track jets associated with the selected large-R jet candidate are b tagged, exploiting the decays of Z and H bosons to a $b\bar{b}$ quark pair together with strong background suppression. A window requirement on the jet mass is also applied. In the $Z\gamma$ search, the mass interval grows from 80–106 GeV for jets with a p_{T} of 500 GeV to 70–110 GeV for jets with a p_{T} of 2.5 TeV. These mass intervals are varied such that an approximately constant signal efficiency across the whole jet p_{T} spectrum is maintained, accounting for the jet mass resolution increase as a function of jet p_{T}. In the $H\gamma$ search, the mass interval is 93–134 GeV independently of the jet p_{T}. In the $Z\gamma$ and $H\gamma$ searches, the jet must also have fewer than 30 associated tracks (n_{trk}) originating from the primary vertex for the event to be accepted in this category. This requirement is made to reject gluon-initiated jets that mimic a two-subjet structure due to gluon splitting [56]. Relative to the baseline selection, the efficiency of selecting in the BTAG category an event originating from a $Z\gamma$ resonance with a mass of 1 TeV, in the hadronic Z boson decay mode, is 3% to 4% depending on the spin hypothesis and production mode, while only 0.02% of background events enter this category for the same mass value. For the $H\gamma$ resonances with a mass of 1 TeV, in the $H \to b\bar{b}$ decay mode, the selection efficiency is 25%. As shown in Fig. 4, the BTAG category becomes ineffective for capturing signal events originating from resonances with masses higher than approximately 3 TeV due to b-tagging inefficiency for highly boosted jets. In the $H\gamma$ search, the categorization process is stopped at this stage, with the remaining events in the baseline selection being rejected from further analysis.

Events not entering the BTAG category in the $Z\gamma$ search and events from the baseline set in the $W\gamma$ search are placed in the D2 category if the selected jet satisfies the combined jet mass and $D_2^{(\beta=1)}$ discriminant requirements. In the $W\gamma$ search, the $n_{\mathrm{trk}} < 30$ requirement must also be satisfied. The mass window requirement in the $Z\gamma$ search is the same as in the BTAG category. In the $W\gamma$ search, the mass interval grows from 71–95 GeV for jets with a p_{T} of 500 GeV to 60–100 GeV for jets with a p_{T} of 2.5 TeV. Approximately 20% to 25% (depending on the spin hypothesis and the production mode) of 1 TeV $Z\gamma$ resonance decays passing the baseline selection enter this category with the fraction increasing to 22%–28% for 4 TeV resonances. For the $W\gamma$ decays, the fraction is approximately 40% for m_X below 4 TeV. The difference in the D2 categorization efficiency between the $Z\gamma$ and $W\gamma$ processes is explained by differences between the angular distributions of the Z and W boson decay products due to the longitudinal polarization of the

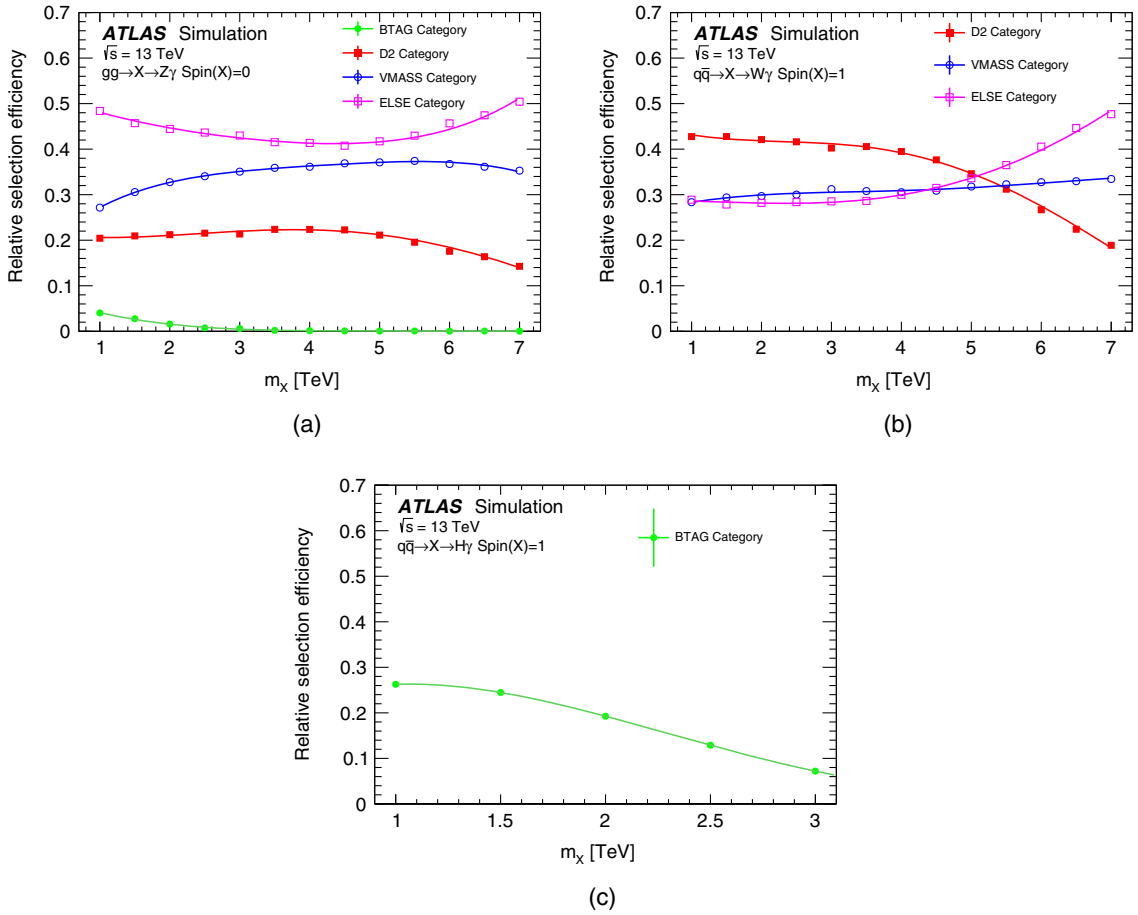

FIG. 4. Efficiencies relative to the baseline selection for signal events to pass the category selection for (a) the $Z\gamma$ (in the spin-0 production hypothesis), (b) the $W\gamma$, and (c) the $H\gamma$ resonances as a function of the resonance mass m_X. The lines represent polynomial fits to the simulated data points. In the $Z\gamma$ search, the categorization efficiencies have only a small dependence on the production and spin hypotheses. Statistical uncertainties are smaller than the marker size.

W boson and transverse polarization of the Z boson. For both the $Z\gamma$ and $W\gamma$ resonances, the D2 categorization efficiency decreases for m_X above 4 TeV, as shown in Fig. 4, due to the falling discriminating power of the $D_2^{(\beta=1)}$ variable. Only approximately 1% (0.5%) of background events passing the baseline selection for resonance masses of 1 TeV (4 TeV) enter this category.

Events that fail to enter either of the first two categories and only pass the jet mass selection enter the VMASS category. The efficiency to enter this category, relative to the baseline selection, is 24% to 27% for $Z\gamma$ events from a resonance at 1 TeV, growing to 35%–36% for a resonance at 4 TeV, and approximately 30% for $W\gamma$ events. Approximately 9% of the background events enter this category after passing the baseline selection.

Finally, the remaining events passing the baseline selection are assigned to the ELSE category. The $Z\gamma$ resonance events enter this category with an efficiency of 40% to 50%, and $W\gamma$ events enter with approximately 30% efficiency for resonances below 4 TeV, growing to 50% for a resonance at 7 TeV.

V. SIGNAL AND BACKGROUND MODELS

The final discrimination between signal and background events in the selected samples is achieved with a fit of a signal + background model to the $m_{J\gamma}$ distribution of the selected data events. The fit relies on the parametrization of signal and background $m_{J\gamma}$ distributions with a functional form.

A. Signal model

The shape of the $m_{J\gamma}$ distribution is modeled by the sum of a crystal ball function [57] representing the core populated by well-reconstructed events and a Gaussian function modeling the tails populated by poorly reconstructed events as described by Eq. (1),

$$S(m_{J\gamma}) = f_{\mathcal{C}} \cdot \mathcal{C}(m_{J\gamma}; \mu, \sigma_{\mathcal{C}}, \alpha_{\mathcal{C}}, n_{\mathcal{C}}) + (1 - f_{\mathcal{C}}) \cdot \mathcal{G}(m_{J\gamma}; \mu, \sigma_{\mathcal{G}}), \quad (1)$$

where $\mathcal{C}$ is the crystal ball function defined by Eq. (2),

$$\mathcal{C}(m_{J\gamma};\mu,\sigma_{\mathcal{C}},\alpha_{\mathcal{C}},n_{\mathcal{C}}) = N_{\mathcal{C}}\cdot\begin{cases}\exp\left(-\frac{(m_{J\gamma}-\mu)^2}{2\sigma_{\mathcal{C}}^2}\right) & \text{for } \frac{m_{J\gamma}-\mu}{\sigma_{\mathcal{C}}} > -\alpha_{\mathcal{C}} \\ \left(\frac{n_{\mathcal{C}}}{\alpha_{\mathcal{C}}}\right)^{n_{\mathcal{C}}}\exp\left(-\frac{\alpha_{\mathcal{C}}^2}{2}\right)\left(\frac{n_{\mathcal{C}}}{\alpha_{\mathcal{C}}}-\alpha_{\mathcal{C}}-\frac{m_{J\gamma}-\mu}{\sigma_{\mathcal{C}}}\right)^{-n_{\mathcal{C}}} & \text{for } \frac{m_{J\gamma}-\mu}{\sigma_{\mathcal{C}}} \leq -\alpha_{\mathcal{C}}\end{cases}, \quad (2)$$

and $\mathcal{G}$ is a Gaussian function with mean μ and standard deviation $\sigma_{\mathcal{G}}$. The normalization factor $N_{\mathcal{C}}$ depends on the shape parameters of the crystal ball function. The relative strength of the two distributions, $f_{\mathcal{C}}$, is a parameter of the signal description model. Since the modeling of the tails of the mass peak is addressed by the Gaussian function, the parameter $n_{\mathcal{C}}$, controlling the shape of the tail of the crystal ball function, is fixed to 1. Similarly, the parameter $\alpha_{\mathcal{C}}$, designating the onset of the power law tail of the crystal ball function is constrained to be between 0 and 4. Additional free parameters $\sigma_{\mathcal{C}}$ and $\sigma_{\mathcal{G}}$ describe the widths of the crystal ball and the Gaussian distributions corresponding to the width of the core of the $m_{J\gamma}$ distribution and the width of the tails.

The model described above is fitted to the $m_{J\gamma}$ distribution of simulated events of each signal type considered, for m_X ranging from 850 GeV to 7 TeV, for each category. To obtain a model varying continuously as a function of the resonance mass, the parameters are interpolated using polynomials of up to the third degree. For all signal hypotheses, $\sigma_{\mathcal{C}}$ is about 20 GeV for a 1 TeV resonance and grows linearly by 15 GeV per 1 TeV increase of the resonance mass.

B. Background model

Several SM processes contribute to the predicted event yield with different proportions. In the BTAG category, the dominant SM process is photon production in association with a b-flavored hadron, whereas in the other categories, photon production in association with a light or c-flavored hadron dominates. The production of a photon in association with a Z or W boson or the pair production of top quarks also contributes to the total background. For events with $m_{J\gamma} > 1$ TeV, the contribution in the BTAG category from $\gamma + Z$ production is approximately 32% (13%) for the $Z\gamma$ ($H\gamma$) search, while in the D2 category, the contribution from $\gamma + W/Z$ production is approximately 15% for both the $Z\gamma$ and $W\gamma$ searches. For other categories, the contributions from SM $\gamma + W/Z$ production are below 5%.

Samples of simulated events arising from the processes described above are used to develop the functional modeling of the background and to test the applicability of the functional form, number of parameters, and range of the fit. Multijet production, where one jet is reconstructed as a photon, also contributes to the event samples. The contribution of this type of events is estimated using a data-driven method [8] and shown to be about 10% of the events passing the baseline selection and to not affect the $m_{J\gamma}$ distribution. Multijet production is therefore accounted for in the background model through the γ + jet production.

The family of functions from Ref. [58], as described by Eq. (3), with up to five parameters, is used for the overall background model

$$B(m_{J\gamma};\boldsymbol{p}) = (1-x)^{p_1}x^{p_2+p_3\log(x)+p_4\log^2(x)+p_5\log^3(x)}, \quad (3)$$

where x is $m_{J\gamma}$ divided by the collision energy and $\boldsymbol{p} \equiv (p_1, p_2, p_3, p_4, p_5)$ is the vector of shape parameters. In the VMASS and D2 categories, the fit spans the $m_{J\gamma}$ range of 800 GeV to 7 TeV; in the BTAG category, it spans the range from 800 GeV to 3.2 TeV; and in the ELSE category, it spans the range from 2.5 to 7 TeV.

The number of parameters p_i used in the model is chosen by testing the stability of the fit and the ability of the function to describe the $m_{J\gamma}$ background distributions over the range expected for the different event categories. The MC-simulated backgrounds inside the signal region are used in these tests, and data outside the signal region are used to validate the functional form choice for the background model. The complementary data set selection follows the categorization procedure described in Sec. IV with the exception that the photon candidates are required to satisfy $1.52 < |\eta| < 2.37$. The model also uses an F-test statistic [59] to decide on the minimum number of parameters required. The number of model parameters p_i varies from two to three depending on the event category. The background modeling is stable while varying the relative fractions of the contributing SM processes. Ensemble tests with pseudodata are used to validate the background model in regions of the $m_{J\gamma}$ distributions poorly populated by the data events. The ensemble tests are performed separately in different categories for each of the $Z\gamma$, $W\gamma$, and $H\gamma$ searches. Simulated event samples from SM processes are used to generate the pseudodata. In addition ensemble tests are performed, where a signal process at the level of sensitivity of this search is also included in the simulated data.

VI. SYSTEMATIC UNCERTAINTIES

Uncertainties from systematic effects are due to the background estimation as well as the detector modeling,

which affect the shape and normalization of the signal $m_{\mathrm{J}\gamma}$ distributions. These effects are estimated as relative uncertainties for the signal efficiency and the position and width of the signal peak for resonance masses ranging from 1 to 7 TeV in 500 GeV steps. The impact of these effects on the $m_{\mathrm{J}\gamma}$ distribution is evaluated using simulation. Third-order polynomial interpolations are used to obtain relative variations of the signal efficiency and shape parameters due to each systematic uncertainty, for an arbitrary value of the resonance mass.

A. Uncertainty in background estimate

A systematic uncertainty associated with the background description arises from a potential bias in the estimated number of signal events due to the functional form chosen for the background parametrization described by Eq. (3). This effect, referred to as the spurious signal (N_{spur}), is studied using simulated background events (including $\gamma +$ jet and $W/Z +$ jet). The bias is estimated by fitting the signal-plus-background model to simulated background $m_{\mathrm{J}\gamma}$ distributions in each event category, for each signal hypothesis, with the sample's statistical uncertainties as expected in the data. The absolute number of fitted signal events at a given m_X hypothesis defines the number of spurious signal events $N_{\mathrm{spur}}(m_X)$. The impact of uncertainties in the background composition has been studied by varying the fraction of the $W/Z +$ jet and $\gamma + b/c$ jet backgrounds by 50% and found to be negligible in the spurious signal estimate. The impact of the spurious signal uncertainty on the exclusion limits is discussed in Sec. VIII.

B. Luminosity

An integrated luminosity uncertainty of 2.1% is derived, following a methodology similar to that detailed in Ref. [60], from a calibration using beam separation scans performed in August 2015 and May 2016.

C. Jet energy scale and resolution

The uncertainties in the jet energy scale and resolution are estimated using $\gamma +$ jet and dijet events in the data [46].

The impact of the systematic uncertainty in the jet energy scale is a shift of the peak position of the signal $m_{\mathrm{J}\gamma}$ distribution by 1%–3%. The signal mass resolution varies by 5% in the low-mass region ($m_X < 2.5$ TeV) and by 15% in the high-mass region due to the systematic uncertainty in the jet energy resolution. The impact on the signal efficiency from the jet energy uncertainty is 2%–6%.

D. Photon energy scale and resolution

The uncertainties in the photon energy scale and resolution are estimated using electron data samples with $Z \to ee$ events and high-purity photon samples with radiative $Z \to ee\gamma$ events [41]. The impact of the systematic uncertainty in the photon energy scale is a shift of 0.5% in the peak position of the signal $m_{\mathrm{J}\gamma}$ distribution. The signal mass resolution varies by 1% in the low-mass region and by 3% in the high-mass region due to the systematic uncertainty in the photon energy resolution.

E. Photon identification, isolation, and trigger efficiency

The uncertainties in the reconstruction, identification, isolation, and trigger efficiency for photons are determined from data samples of $Z \to \ell\ell\gamma$, $Z \to ee$, and inclusive photon events, using the methods described in Ref. [19]. The impact on the signal efficiency from the photon identification, isolation, and trigger systematic uncertainties is found to be less than 1.5%, 0.5%, and 0.1%, respectively.

F. Heavy-flavor jet identification

Uncertainties in the b-tagging efficiency for track jets are derived from the uncertainties measured in dedicated heavy-flavor-enriched data samples, following the methodology described in Ref. [54]. The uncertainties are measured as a function of b-jet p_{T} and range between 2% and 8% for track jets with $p_{\mathrm{T}} < 250$ GeV. For track jets with $p_{\mathrm{T}} > 250$ GeV, the uncertainty in the tagging efficiencies is extrapolated using simulation [54] and is approximately 9% for track jets with $p_{\mathrm{T}} > 400$ GeV. The impact of these uncertainties on the signal efficiency is 10%–20%.

TABLE I. Effect of systematic uncertainties from various sources on signal normalization and efficiency, position of the signal peak, and the core width σ_C of the signal peak. The last two rows show the theoretical uncertainty effects on the signal acceptances.

	Impact on normalization and efficiency (%)
Luminosity	2.1
Jet energy scale	2–6
Photon identification and isolation	0.5–1.5
Flavor tagging	10–20
n_{trk} associated with the jet	6
Jet mass resolution	3–6
$D_2^{(\beta=1)}$ scale and resolution	<1
Pileup modeling	1–2
	Impact on signal peak position (%)
Jet energy and mass scale	1–3
Photon energy scale	<0.5
	Impact on signal peak resolution (%)
Jet energy resolution	5($m_X < 2.5$ TeV)–15($m_X > 2.5$ TeV)
Photon energy resolution	1–3
	Impact on acceptance (%)
PDF	2–12
Parton shower	2

TABLE II. Event yields in the baseline selection and in the $Z\gamma$, $W\gamma$, and the $H\gamma$ searches, in the categories used in those searches. Only events with $m_{J\gamma} > 1$ TeV are considered.

	Event yield in each category ($m_{J\gamma} > 1$ TeV)				
Selection	Baseline	BTAG	D2	VMASS	ELSE
$Z\gamma$ search	60,237	25	784	5,569	53,859
$W\gamma$ search	60,237	⋯	661	5,216	54,360
$H\gamma$ search	60,237	59	⋯	⋯	⋯

G. Number of primary-vertex-originated tracks associated with the jet

The requirement on the number of tracks originating from the primary vertex and associated with the jet induces a 6% systematic uncertainty in the signal efficiency, as estimated from the comparison of data control samples and samples of simulated events [56].

H. Scale and resolution of the jet mass and $D_2^{(\beta=1)}$

The uncertainties in the scale and resolution of the jet mass and $D_2^{(\beta=1)}$ are evaluated by comparing

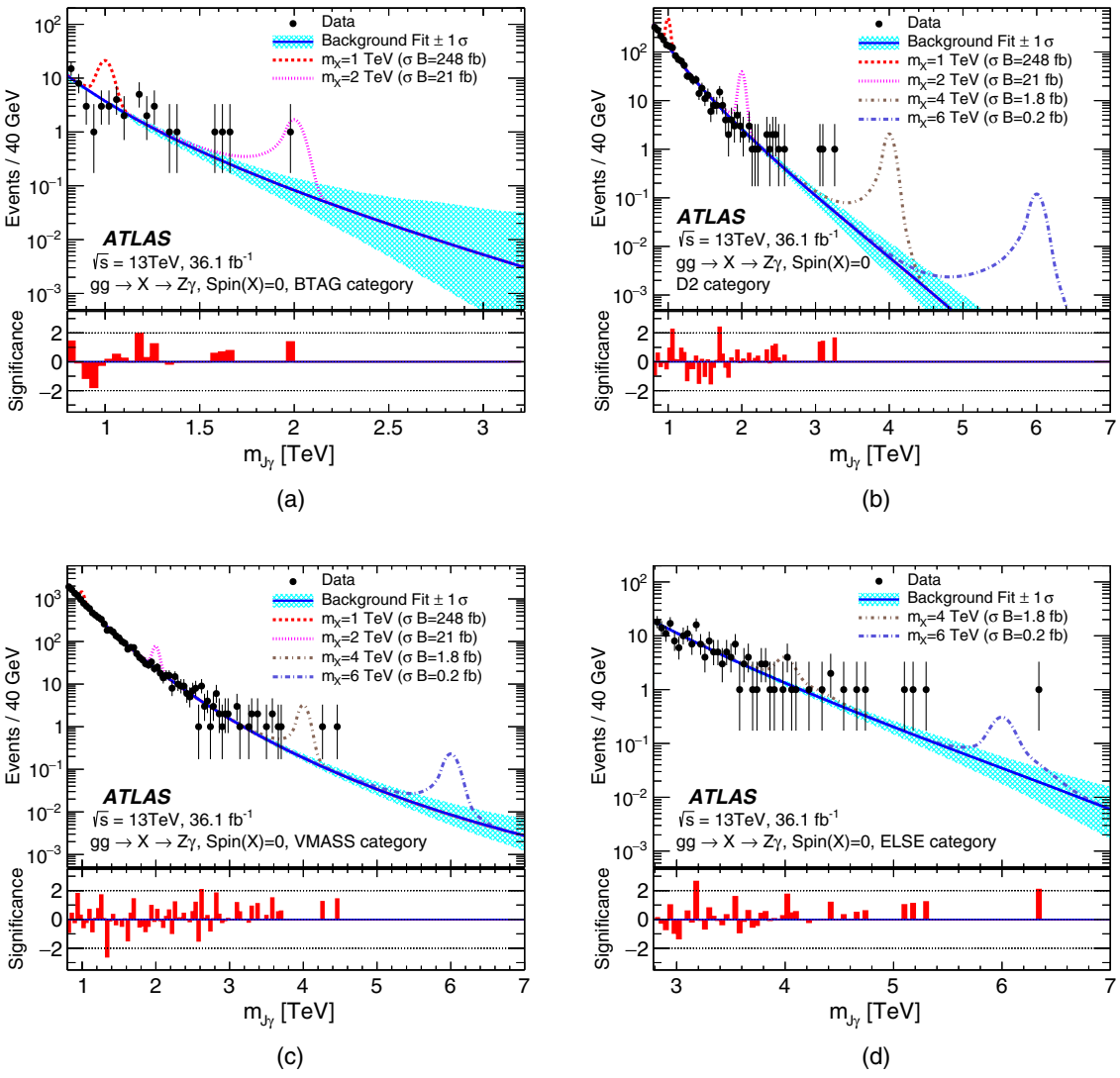

FIG. 5. Distributions of the reconstructed mass $m_{J\gamma}$ in the $Z\gamma$ search (a) BTAG, (b) D2, (c) VMASS, and (d) ELSE categories. The models obtained in the background-only fits are shown by the solid lines. Hypothetical signal distributions with σB at the level excluded multiplied by factors of 20 (for 1 TeV), 10 (for 2 TeV), 5 (for 4 TeV), and 1 (for 6 TeV) for the given signal model and resonance mass are overlaid. The σB lines are calculated with the scale factors applied. The bottom panels give the significance for each bin. The significance calculation assumes that the background estimate in a given bin is Poisson distributed and follows the recommendation of Ref. [69]. The impact on the background fit of the statistical uncertainties in parameters p_i is shown as a light band around the solid line. This effect is incorporated into the significance calculation.

the ratio of the calorimeter-based to the track-based measurements in dijet data and simulation [52,61]. The jet mass resolution uncertainty affects the signal efficiency by 3%–6%. The impact of $D_2^{(\beta=1)}$ scale and resolution uncertainties on the signal efficiency and the core width σ_C of the signal peak is found to be less than 1%.

I. Pileup modeling

The pileup weighting of the simulated signal events, described in Sec. III, is varied to cover the uncertainty in the ratio of the predicted and measured inelastic pp cross sections [62]. The pileup uncertainty affects the signal efficiency by 1%–2%.

J. PDF choice

The uncertainty due to the PDF modeling is evaluated by comparing the signal acceptances for alternative PDF sets to that for the nominal set. The total uncertainty in the acceptance is derived as the standard deviation of the eigenvariations according to the method described in Ref. [63]. The uncertainties in acceptances for signal processes produced via $q\bar{q}$ annihilation vary from 5% to 2% with increasing resonance mass, while for signal processes produced via gluon–gluon fusion, the uncertainties vary from 12% to 2%.

K. Parton shower

The uncertainty due to the parton shower modeling is evaluated by comparing the signal acceptances for

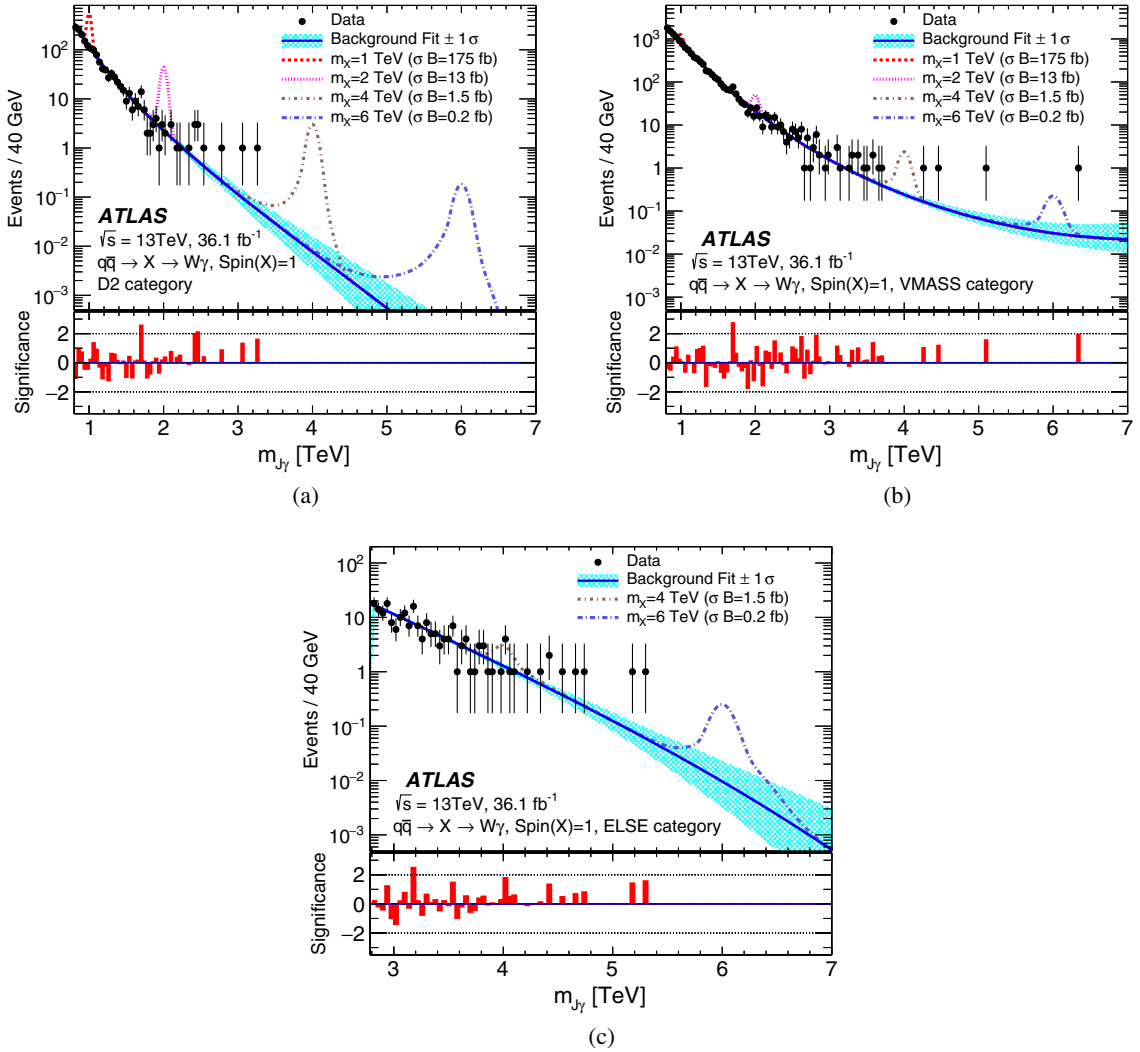

FIG. 6. Distributions of the reconstructed mass $m_{J\gamma}$ in the $W\gamma$ (a) D2, (b) VMASS, and (c) ELSE categories. The models obtained in the background-only fits are shown by the solid lines. Hypothetical signal distributions with σB at the level excluded multiplied by factors of 20 (for 1 TeV), 10 (for 2 TeV), 5 (for 4 TeV), and 1 (for 6 TeV) for the given signal model and resonance mass are overlaid. The σB lines are calculated with the scale factors applied. The bottom panels give the significance for each bin. The significance calculation assumes that the background estimate in a given bin is Poisson distributed. The calculation follows the recommendation of Ref. [69]. The impact on the background fit of the statistical uncertainties in parameters p_i is shown as a light band around the solid line. This effect is incorporated into the significance calculation.

alternative parton shower models to the acceptance for the nominal model. The alternative parton shower models are defined as the eigenvariations of the PYTHIA A14 tune [27]. The total uncertainty is derived as the sum in quadrature of all the eigenvariation effects and affects the acceptance by about 2%.

The effects of systematic shifts on the signal normalization, position of the signal peak, and core width σ_C of the signal peak are summarized in Table I for the $Z\gamma$, $W\gamma$, and $H\gamma$ searches. The effects on the signal acceptances from theoretical uncertainties are also given.

VII. STATISTICAL PROCEDURE

The data are scrutinized with statistical methods to quantify the presence of a hypothetical resonance and to set a limit on its production. In both cases, an unbinned extended maximum likelihood estimator is used to model the data. The parameter of interest is σB_{had}, the signal cross section times the branching fraction of the resonance decaying to $(Z/W/H)\gamma$ with subsequent hadronic $(b\bar{b})$ decays of Z/W (Higgs) bosons. The impact of systematic uncertainties on the signal is modeled with a vector of nuisance parameters, $\boldsymbol{\theta}$, where each component, θ_k, is constrained with corresponding Gaussian probability density functions $\mathcal{G}_k(\theta_k)$. The likelihood model, $\mathcal{L}$, for the sample of data events is described by Eq. (4),

$$\mathcal{L}(\sigma B_{\mathrm{had}}, m_X) = \prod_j \left[\frac{e^{-N_j(\sigma B_{\mathrm{had}},\boldsymbol{\theta})} N_j(\sigma B_{\mathrm{had}},\boldsymbol{\theta})^{n_j}}{n_j!} \times \prod_{\ell} \left(f_{\mathrm{tot},j}(m_{\mathrm{J}\gamma,\ell}; \sigma B_{\mathrm{had}}, \boldsymbol{p}, \boldsymbol{\theta}, m_X) \right) \right] \times \prod_k \mathcal{G}_k(\theta_k), \tag{4}$$

where j represents the event category, n_j is the observed number of events in that category, ℓ is the event index, and $N_j(\sigma B_{\mathrm{had}}, \boldsymbol{\theta})$ is the expected total event yield in category j. The total probability density function $f_{\mathrm{tot},j}$ in category j depends on the photon-jet invariant mass $m_{\mathrm{J}\gamma,\ell}$ and is a function of the parameter of interest σB_{had}, the parameters of the background modeling function $\boldsymbol{p}$, the nuisance parameters θ_k, as well as the mass m_X of the hypothetical resonance. The functional form of $f_{\mathrm{tot},j}$ is given in Eq. (5),

$$f_{\mathrm{tot},j}(m_{\mathrm{J}\gamma,\ell}; \sigma B_{\mathrm{had}}, \boldsymbol{p}, \boldsymbol{\theta}, m_X) = \frac{1}{N_j(\sigma B_{\mathrm{had}}, \boldsymbol{\theta}, \boldsymbol{p})} [(N_{\mathrm{sig},j}(\sigma B_{\mathrm{had}}, \boldsymbol{\theta}, m_X) + N_{\mathrm{spur},j}(\theta_{\mathrm{spur},j}, m_X)) \times S_j(m_{\mathrm{J}\gamma,\ell}; \sigma B_{\mathrm{had}}, \boldsymbol{\theta}) + N_{\mathrm{bkg},j} B_j(m_{\mathrm{J}\gamma,\ell}; \boldsymbol{p}_j)], \tag{5}$$

where S_j and B_j are the signal and background probability density functions in category j, described in Sec. V. The parameter $\theta_{\mathrm{spur},j}$ is an element of the $\boldsymbol{\theta}$ vector corresponding to the spurious signal nuisance parameter. The expected yield of signal events $N_{\mathrm{sig},j}$ is given by the product of σB_{had}, integrated luminosity, acceptance, and efficiency for a given category j. The expected number of background events $N_{\mathrm{bkg},j}$ is a parameter of the fit. The total expected event yield in a given category, N_j, is the sum of the expected signal, background, and spurious signal event yields.

The p values are computed to examine the compatibility of the data and the background-only hypothesis. First, the local p value is calculated for the particular value of m_X under consideration. The local p value is defined as the probability of the background to produce a signal-like excess of which the estimated σB_{had} is larger than that found in the fit to the data in all categories simultaneously. This procedure utilizes the ratio of the likelihood value where the most likely value of the parameter of interest σB_{had} is found to the likelihood value where no signal is allowed ($\sigma B_{\mathrm{had}} = 0$) [64]. The global p value is defined as the probability of finding, at any value of m_X, a signal-like fluctuation more significant than the most significant excess found in the data, in all categories combined. It is calculated approximately by discounting the local p value by the effective number of search trials possible within the $m_{\mathrm{J}\gamma}$ range examined.

The modified frequentist ($\mathrm{CL_s}$) method [65,66] is used to set upper limits on the signal σB_{had} at 95% C.L. To obtain

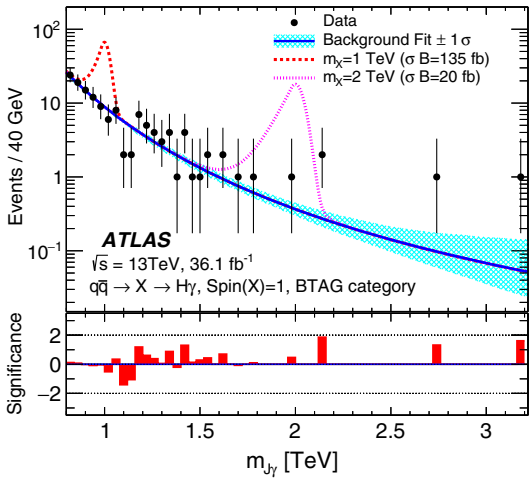

FIG. 7. Distribution of the reconstructed mass $m_{\mathrm{J}\gamma}$ in the $H\gamma$ search BTAG category. The models obtained in the background-only fits are shown by the solid lines. Hypothetical signal distributions with σB at the level excluded multiplied by factors of 20 (for 1 TeV) and 10 (for 2 TeV) for the given signal model and resonance mass are overlaid. The σB lines are calculated with the scale factors applied. The bottom panel gives the significance for each bin. The significance calculation assumes that the background estimate in a given bin is Poisson distributed. The calculation follows the recommendation of Ref. [69]. The impact on the background fit of the statistical uncertainties in parameters p_i is shown as a light band around the solid line. This effect is incorporated into the significance calculation.

limits on σB, which is the signal cross section times the branching fraction of resonance decays to $(Z/W/H)\gamma$ with all allowed decays of Z, W, and Higgs bosons, the resulting σB_{had} is divided by the measured hadronic branching fraction of the Z (69.91% [67]) or W (67.41% [67]) bosons or the theoretically calculated branching fraction of the Higgs boson to $b\bar{b}$ (58.24% [68]).

Closed-form asymptotic formulas [64] are used to calculate the limits. The p value calculation and σB limit calculations are performed for m_{X} in range of 1 to 6.8 TeV in steps of 20 GeV. The step size is chosen to be much smaller than the experimental $m_{\mathrm{J}\gamma}$ resolution, and the interval spans the interpolation range of the shape parameters. The VMASS and D2 categories are used in the entire range, while the BTAG category is used only for 1 TeV $< m_{\mathrm{X}} <$ 3 TeV, and the ELSE category is used only for 3 TeV $< m_{\mathrm{X}} <$ 6.8 TeV. The fit interval described in Sec. V B is selected such that a peak in the $m_{\mathrm{J}\gamma}$ distribution, resulting from resonance with m_{X} considered, is fully contained.

Due to the small number of events for large m_X values, the results are checked with ensemble tests. The limits derived with asymptotic formulas agree well with those

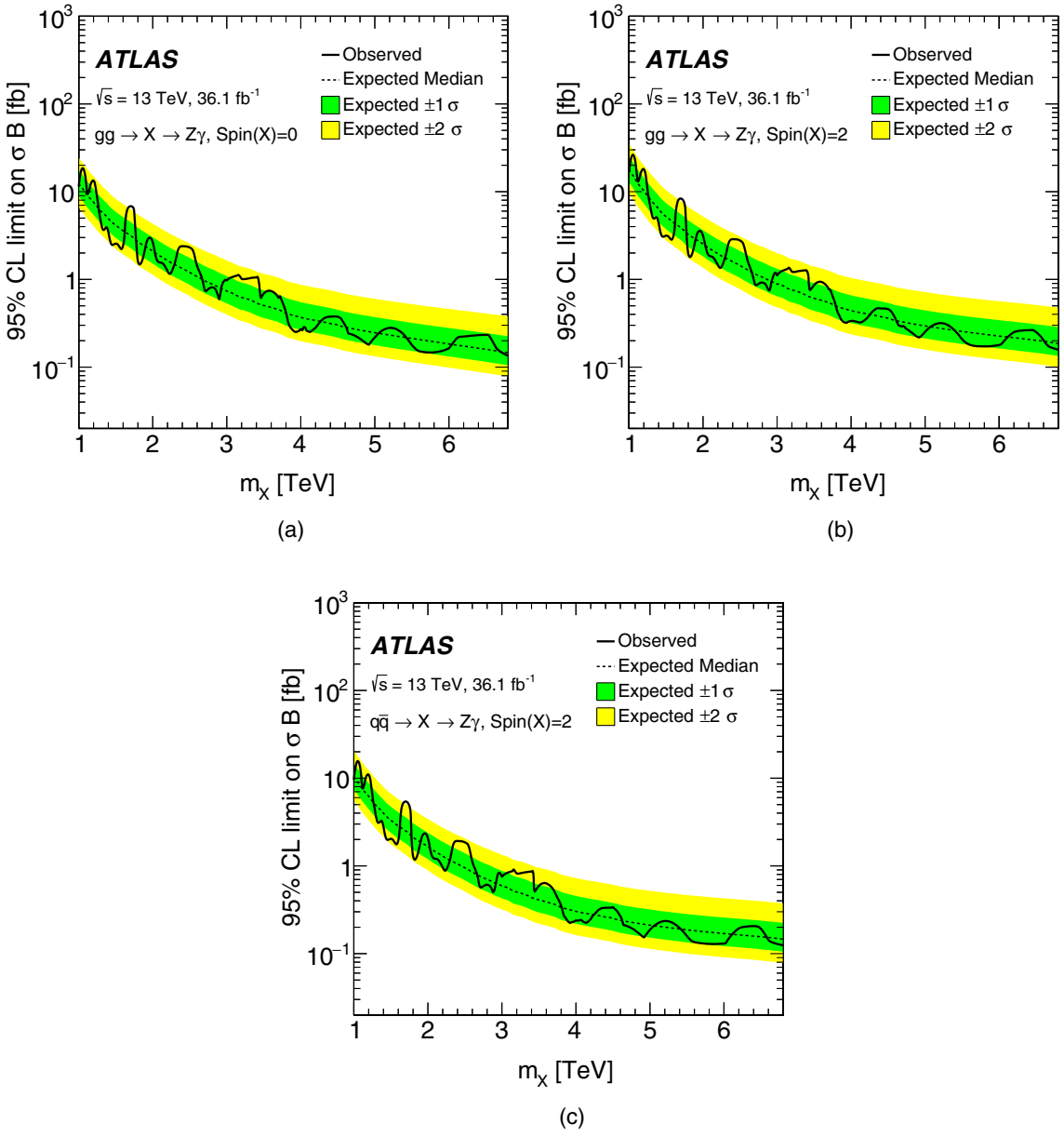

FIG. 8. The 95% C.L. observed (solid line) and expected (dashed line) upper limits on σB for a resonance with (a) spin-0, produced by gluon–gluon fusion; (b) spin-2, produced by gluon–gluon fusion; and (c) spin-2, produced by quark-antiquark annihilation, decaying to $Z\gamma$ as a function of the resonance mass. The inner and outer bands give the ± 1 and ± 2 standard deviations of expected limits. The local deviations of the observed upper limits from the expected ones on σB are a result of small deviations in the data from the best-fitting background-only model.

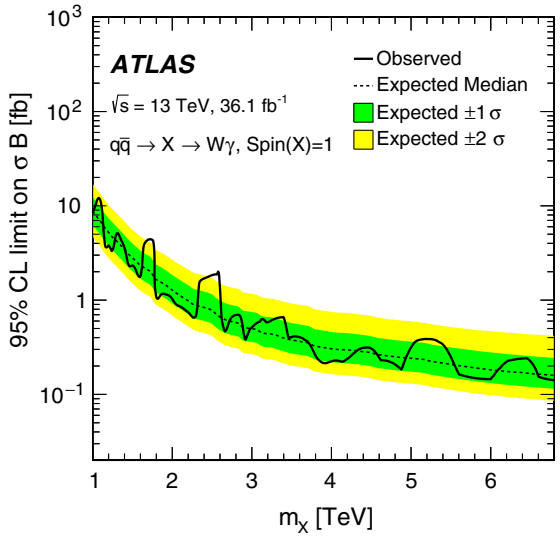

FIG. 9. The 95% C.L. observed (solid line) and expected (dashed line) upper limits on σB for a spin-1 resonance decaying to $W\gamma$ as a function of the resonance mass. The inner and outer bands give the ± 1 and ± 2 standard deviations of expected limits. The local deviations of the observed upper limits from the expected ones on σB are a result of small deviations in the data from the best-fitting background-only model.

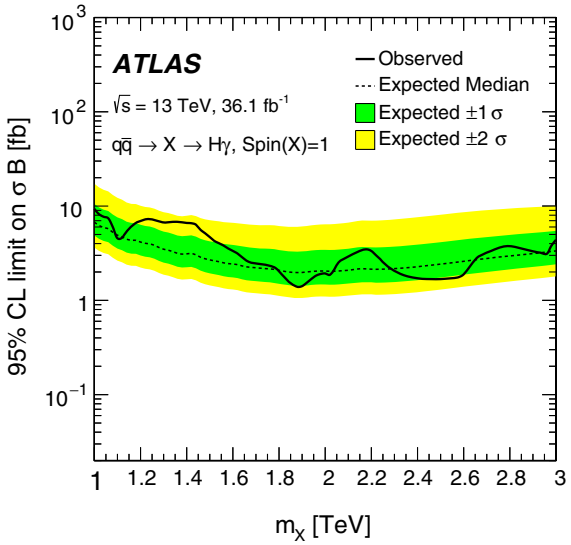

FIG. 10. The 95% C.L. observed (solid line) and expected (dashed line) upper limits on σB for a spin-1 resonance decaying to $H\gamma$ as a function of the resonance mass. The inner and outer bands give the ± 1 and ± 2 standard deviations of expected limits. The local deviations of the observed upper limits from the expected ones on σB are a result of small deviations in the data from the best-fitting background-only model.

obtained with ensemble tests for small m_X values and are underestimated by as much as 30% for large m_X values.

VIII. RESULTS

The data event yields in the baseline selection as well as in all search channels and in the categories within each channel are shown in Table II.

The observed $m_{J\gamma}$ distributions as well as the background distributions obtained from a global background-only fit with various hypothetical signal curves overlaid are shown in Figs. 5–7, for the $Z\gamma$, $W\gamma$, and $H\gamma$ searches, respectively. The event with the highest $m_{J\gamma}$, at a value of 6.3 TeV, has a jet of mass 63 GeV, and it is found in the ELSE (VMASS) category of the $Z\gamma$ ($W\gamma$) search.

The smallest local p value, corresponding to a significance of 2.7σ, is found in the $W\gamma$ search at $m_{J\gamma} = 2.5$ TeV utilizing data from all categories simultaneously. This local p value corresponds to a global significance of less than 1σ. No significant excess is observed in any of the categories and analysis channels. Limits are placed on specific models.

The σB limits on $Z\gamma$ production, evaluated for resonance masses between 1.0 and 6.8 TeV, are shown in Fig. 8. Spin and production hypotheses comprise a spin-0 resonance, produced by gluon–gluon fusion and a spin-2 resonance, produced by gluon–gluon fusion and $q\bar{q}$ annihilation. The σB limit on $W\gamma$ resonances evaluated for m_X between 1 and 6.8 TeV are shown in Fig. 9. This is the first evaluation of such a limit utilizing hadronic W boson decays. The $Z\gamma$ and $W\gamma$ limits decrease from approximately 10 fb for a resonance mass of 1 TeV to 0.1 fb for a resonance mass of 6.8 TeV. The $H\gamma$ search presented here is the first search for a heavy resonance with this decay mode. The σB limits on the resonances decaying to a $H\gamma$ final state are shown in Fig. 10. The limit is evaluated for resonance masses between 1 and 3 TeV and varies between 10 and 4 fb depending on m_X. The limit weakens for $m_X > 2$ TeV due to a decrease in signal efficiency as shown in Fig. 4, stemming from the decrease in the b-tagging efficiency for high-momentum jets.

The sensitivity of the resonance search and the strength of the resonance production cross section limit are primarily determined by the available data sample size. Among all the systematic uncertainties, the spurious-signal uncertainty on the background estimation has the largest impact on the limit, in particular in the low-mass region, weakening the limit by up to 20% (1%) at $m_X = 1$ TeV (6.8 TeV). Another important systematic uncertainty is that in the heavy-flavor jet identification efficiency. It weakens the limit by up to 13% (20%) at $m_X = 1$ TeV (3 TeV) in the $H\gamma$ analysis, while it has little impact on the limits in the $Z\gamma$ analysis since the BTAG category is just one of the four categories in this analysis.

IX. CONCLUSION

Results are presented from a search for heavy resonances decaying to $Z\gamma$, $W\gamma$, or $H\gamma$ final states using 36.1 fb^{-1} of $\sqrt{s} = 13$ TeV pp collision data collected by the ATLAS

experiment during the 2015 and 2016 run periods of the LHC. The search sensitivity is enhanced for high-mass resonances by selecting hadronic decays of the Z and W bosons and the $b\bar{b}$ decay of the Higgs boson, identified as large-radius jets. Distributions of the invariant mass of photon-jet pairs are used to search for resonances in the mass range from 1.0 to 6.8 TeV for decays to $Z\gamma$ and $W\gamma$ and between 1.0 and 3.0 TeV for decays to $H\gamma$. No evidence for new resonances is found, and limits are set based on assumptions about the spin and production model of the resonance.

The 95% confidence level upper limits on the resonance production cross section times decay branching fraction to $Z\gamma$ and $W\gamma$ final states vary from about 10 to 0.1 fb for masses from 1.0 to 6.8 TeV, with individual studies carried out for resonances with spin 0, 1, and 2 produced via gluon-gluon fusion and $q\bar{q}$ annihilation. For the spin-1 $X \to H\gamma$ search, the limits vary from about 10 to 4 fb for resonance masses between 1.0 and 3.0 TeV. These results set the first limits on the production of $H\gamma$ resonances, and this search covers a wider mass range and has a broader scope than previous searches for heavy resonances decaying to $Z\gamma$ and $W\gamma$ final states.

ACKNOWLEDGMENTS

We thank CERN for the very successful operation of the LHC, as well as the support staff from our institutions without whom ATLAS could not be operated efficiently. We acknowledge the support of ANPCyT, Argentina; YerPhI, Armenia; ARC, Australia; BMWFW and FWF, Austria; ANAS, Azerbaijan; SSTC, Belarus; CNPq and FAPESP, Brazil; NSERC, NRC, and CFI, Canada; CERN; CONICYT, Chile; CAS, MOST, and NSFC, China; COLCIENCIAS, Colombia; MSMT CR, MPO CR, and VSC CR, Czech Republic; DNRF and DNSRC, Denmark; IN2P3-CNRS, CEA-DRF/IRFU, France; SRNSFG, Georgia; BMBF, HGF, and MPG, Germany; GSRT, Greece; RGC, Hong Kong SAR, China; ISF, I-CORE and Benoziyo Center, Israel; INFN, Italy; MEXT and JSPS, Japan; CNRST, Morocco; NWO, Netherlands; RCN, Norway; MNiSW and NCN, Poland; FCT, Portugal; MNE/IFA, Romania; MES of Russia and NRC KI, Russian Federation; JINR; MESTD, Serbia; MSSR, Slovakia; ARRS and MIZŠ, Slovenia; DST/NRF, South Africa; MINECO, Spain; SRC and Wallenberg Foundation, Sweden; SERI, SNSF, and Cantons of Bern and Geneva, Switzerland; MOST, Taiwan; TAEK, Turkey; STFC, United Kingdom; and DOE and NSF, United States of America. In addition, individual groups and members have received support from BCKDF, the Canada Council, CANARIE, CRC, Compute Canada, FQRNT, and the Ontario Innovation Trust, Canada; EPLANET, ERC, ERDF, FP7, Horizon 2020, and Marie Skłodowska-Curie Actions, European Union; Investissements d'Avenir Labex and Idex, ANR, Région Auvergne, and Fondation Partager le Savoir, France; DFG and AvH Foundation, Germany; Herakleitos, Thales, and Aristeia programs cofinanced by EU-ESF and the Greek NSRF; BSF, GIF, and Minerva, Israel; BRF, Norway; CERCA Programme Generalitat de Catalunya, Generalitat Valenciana, Spain; and the Royal Society and Leverhulme Trust, United Kingdom. The crucial computing support from all WLCG partners is acknowledged gratefully, in particular CERN; the ATLAS Tier-1 facilities at TRIUMF (Canada), NDGF (Denmark, Norway, and Sweden), CC-IN2P3 (France), KIT/GridKA (Germany), INFN-CNAF (Italy), NL-T1 (Netherlands), PIC (Spain), ASGC (Taiwan), RAL (UK), and BNL (USA); and the Tier-2 facilities worldwide and large non-WLCG resource providers. Major contributors of computing resources are listed in Ref. [70].

[1] E. Eichten and K. Lane, Low-scale technicolor at the Tevatron and LHC, Phys. Lett. B **669**, 235 (2008).
[2] N. Arkani-Hamed, A. G. Cohen, and H. Georgi, Electroweak symmetry breaking from dimensional deconstruction, Phys. Lett. B **513**, 232 (2001).
[3] I. Low, J. Lykken, and G. Shaughnessy, Singlet scalars as Higgs imposters at the Large Hadron Collider, Phys. Rev. D **84**, 035027 (2011).
[4] B. A. Dobrescu, P. J. Fox, and J. Kearney, Higgs–photon resonances, Eur. Phys. J. C **77**, 704 (2017).
[5] D0 Collaboration, Search for a scalar or vector particle decaying into $Z\gamma$ in $p\bar{p}$ collisions at $\sqrt{s} = 1.96$ TeV, Phys. Lett. B **671**, 349 (2009).
[6] ATLAS Collaboration, Measurements of $W\gamma$ and $Z\gamma$ production in pp collisions at $\sqrt{s} = 7$ TeV with the ATLAS detector at the LHC, Phys. Rev. D **87**, 112003 (2013); Erratum, Phys. Rev. D**91**, 119901 (2015).
[7] ATLAS Collaboration, Search for new resonances in $W\gamma$ and $Z\gamma$ final states in pp collisions at $\sqrt{s} = 8$ TeV with the ATLAS Detector, Phys. Lett. B **738**, 428 (2014).
[8] ATLAS Collaboration, Search for heavy resonances decaying to a Z boson and a photon in pp collisions at $\sqrt{s} = 13$ TeV with the ATLAS detector, Phys. Lett. B **764**, 11 (2017).
[9] ATLAS Collaboration, Searches for the $Z\gamma$ decay mode of the Higgs boson and for new high-mass resonances in pp collisions at $\sqrt{s} = 13$ TeV with the ATLAS detector, J. High Energy Phys. 10 (2017) 112.
[10] ATLAS Collaboration, Search for dark matter at $\sqrt{s} = 13$ TeV in final states containing an energetic photon and

large missing transverse momentum with the ATLAS detector, Eur. Phys. J. C **77**, 393 (2017).
[11] CMS Collaboration, Search for a Higgs boson decaying into a Z and a photon in pp collisions at $\sqrt{s} = 7$ and 8 TeV, Phys. Lett. B **726**, 587 (2013).
[12] CMS Collaboration, Search for high-mass $Z\gamma$ resonances in $e^+e^-\gamma$ and $\mu^+\mu^-\gamma$ final states in proton–proton collisions at $\sqrt{s} = 8$ and 13 TeV, J. High Energy Phys. 01 (2017) 076.
[13] CMS Collaboration, Search for high-mass $Z\gamma$ resonances in proton–proton collisions at $\sqrt{s} = 8$ and 13 TeV using jet substructure techniques, Phys. Lett. B **772**, 363 (2017).
[14] CMS Collaboration, Search for $Z\gamma$ resonances using leptonic and hadronic final states in proton–proton collisions at $\sqrt{s} = 13$ TeV, arXiv:1712.03143.
[15] P. Artoisenet *et al.*, A framework for Higgs characterisation, J. High Energy Phys. 11 (2013) 043.
[16] D. Pappadopulo, A. Thamm, R. Torre, and A. Wulzer, Heavy vector triplets: Bridging theory and data, J. High Energy Phys. 09 (2014) 060.
[17] ATLAS Collaboration, The ATLAS Experiment at the CERN Large Hadron Collider, J. Instrum. **3**, S08003 (2008).
[18] ATLAS Collaboration, Performance of the ATLAS Trigger System in 2015, Eur. Phys. J. C **77**, 317 (2017).
[19] ATLAS Collaboration, Measurement of the photon identification efficiencies with the ATLAS detector using LHC Run-1 data, Eur. Phys. J. C **76**, 666 (2016).
[20] S. Alioli, P. Nason, C. Oleari, and E. Re, A general framework for implementing NLO calculations in shower Monte Carlo programs: the POWHEG BOX, J. High Energy Phys. 06 (2010) 043.
[21] E. Bagnaschi, G. Degrassi, P. Slavich, and A. Vicini, Higgs production via gluon fusion in the POWHEG approach in the SM and in the MSSM, J. High Energy Phys. 02 (2012) 088.
[22] H.-L. Lai, M. Guzzi, J. Huston, Z. Li, P. M. Nadolsky, J. Pumplin, and C.-P. Yuan, New parton distributions for collider physics, Phys. Rev. D **82**, 074024 (2010).
[23] T. Sjöstrand, S. Mrenna, and P. Z. Skands, A brief introduction to PYTHIA 8.1, Comput. Phys. Commun. **178**, 852 (2008).
[24] J. Pumplin, D. R. Stump, J. Huston, H.-L. Lai, P. Nadolsky, and W.-K. Tung, New generation of parton distributions with uncertainties from global QCD analysis, J. High Energy Phys. 07 (2002) 012.
[25] ATLAS Collaboration, Measurement of the Z/γ^* boson transverse momentum distribution in pp collisions at $\sqrt{s} =$ 7 TeV with the ATLAS detector, J. High Energy Phys. 09 (2014) 145.
[26] J. Alwall, R. Frederix, S. Frixione, V. Hirschi, F. Maltoni, O. Mattelaer, H.-S. Shao, T. Stelzer, P. Torrielli, and M. Zaro, The automated computation of tree-level and next-to-leading order differential cross sections, and their matching to parton shower simulations, J. High Energy Phys. 07 (2014) 079.
[27] ATLAS Collaboration, ATLAS Pythia 8 tunes to 7 TeV data, Report No. ATL-PHYS-PUB-2014-021, 2014, https://cds.cern.ch/record/1966419.
[28] R. D. Ball *et al.*, Parton distributions with LHC data, Nucl. Phys. **B867**, 244 (2013).
[29] T. Gleisberg, S. Höche, F. Krauss, M. Schönherr, S. Schumann, F. Siegert, and J. Winter, Event generation with SHERPA 1.1, J. High Energy Phys. 02 (2009) 007.
[30] S. Schumann and F. Krauss, A parton shower algorithm based on Catani-Seymour dipole factorisation, J. High Energy Phys. 03 (2008) 038.
[31] S. Höche, F. Krauss, S. Schumann, and F. Siegert, QCD matrix elements and truncated showers, J. High Energy Phys. 05 (2009) 053.
[32] T. Gleisberg and S. Höche, Comix, a new matrix element generator, J. High Energy Phys. 12 (2008) 039.
[33] F. Cascioli, P. Maierhöfer, and S. Pozzorini, Scattering Amplitudes with Open Loops, Phys. Rev. Lett. **108**, 111601 (2012).
[34] S. Höche, F. Krauss, M. Schönherr, and F. Siegert, QCD matrix elements + parton showers: The NLO case, J. High Energy Phys. 04 (2013) 027.
[35] D. J. Lange, The EvtGen particle decay simulation package, Nucl. Instrum. Methods Phys. Res., Sect. A **462**, 152 (2001).
[36] S. Agostinelli *et al.*, GEANT4: A simulation toolkit, Nucl. Instrum. Methods Phys. Res., Sect. A **506**, 250 (2003).
[37] ATLAS Collaboration, The ATLAS Simulation Infrastructure, Eur. Phys. J. C **70**, 823 (2010).
[38] ATLAS Collaboration, Summary of ATLAS Pythia 8 tunes, Report No. ATL-PHYS-PUB-2012-003, 2012, https://cds.cern.ch/record/1474107.
[39] A. D. Martin, W. J. Stirling, R. S. Thorne, and G. Watt, Parton distributions for the LHC, Eur. Phys. J. C **63**, 189 (2009).
[40] ATLAS Collaboration, Photon identification in 2015 ATLAS data, Report No. ATL-PHYS-PUB-2016-014, 2016, https://cds.cern.ch/record/2203125.
[41] ATLAS Collaboration, Electron and photon energy calibration with the ATLAS detector using data collected in 2015 at $\sqrt{s} = 13$ TeV, Report No. ATL-PHYS-PUB-2016-015, 2016, https://cds.cern.ch/record/2203514.
[42] ATLAS Collaboration, Topological cell clustering in the ATLAS calorimeters and its performance in LHC Run 1, Eur. Phys. J. C **77**, 490 (2017).
[43] M. Cacciari, G. P. Salam, and G. Soyez, The anti-k_t jet clustering algorithm, J. High Energy Phys. 04 (2008) 063.
[44] D. Krohn, J. Thaler, and L.-T. Wang, Jet trimming, J. High Energy Phys. 02 (2010) 084.
[45] ATLAS Collaboration, Jet energy scale measurements and their systematic uncertainties in proton–proton collisions at $\sqrt{s} = 13$ TeV with the ATLAS detector, Phys. Rev. D **96**, 072002 (2017).
[46] ATLAS Collaboration, In-situ measurements of the ATLAS large-radius jet response in 13 TeV pp collisions, Report No. ATLAS-CONF-2017-063, 2017, https://cds.cern.ch/record/2275655.
[47] ATLAS Collaboration, Jet mass reconstruction with the ATLAS Detector in early Run 2 data, Report No. ATLAS-CONF-2016-035, 2016, https://cds.cern.ch/record/2200211.
[48] M. Cacciari and G. P. Salam, Pileup subtraction using jet areas, Phys. Lett. B **659**, 119 (2008).
[49] ATLAS Collaboration, Reconstruction of primary vertices at the ATLAS experiment in Run 1 proton–proton collisions at the LHC, Eur. Phys. J. C **77**, 332 (2017).
[50] A. J. Larkoski, I. Moult, and D. Neill, Power counting to better jet observables, J. High Energy Phys. 12 (2014) 009.

[51] A. J. Larkoski, G. P. Salam, and J. Thaler, Energy correlation functions for jet substructure, J. High Energy Phys. 06 (2013) 108.
[52] ATLAS Collaboration, Identification of boosted, hadronically-decaying W and Z bosons in $\sqrt{s} = 13$ TeV Monte Carlo simulations for ATLAS, Report No. ATL-PHYS-PUB-2015-033, 2015, https://cds.cern.ch/record/2041461.
[53] ATLAS Collaboration, Performance of jet substructure techniques in early $\sqrt{s} = 13$ TeV pp collisions with the ATLAS detector, Report No. ATLAS-CONF-2015-035, 2015, https://cds.cern.ch/record/2041462.
[54] ATLAS Collaboration, Performance of b-jet identification in the ATLAS experiment, J. Instrum. **11**, P04008 (2016).
[55] ATLAS Collaboration, Optimisation of the ATLAS b-tagging performance for the 2016 LHC Run, Report No. ATL-PHYS-PUB-2016-012, 2016, https://cds.cern.ch/record/2160731.
[56] ATLAS Collaboration, Search for diboson resonances with boson-tagged jets in pp collisions at $\sqrt{s} = 13$ TeV with the ATLAS detector, Phys. Lett. B **777**, 91 (2018).
[57] M. Oreglia, A study of the reactions $\psi' \to \gamma\gamma\psi$, Ph.D. thesis SLAC-R-236, Stanford Linear Accelerator Center, 1980.
[58] ATLAS Collaboration, Search for new phenomena in dijet mass and angular distributions from pp collisions at $\sqrt{s} =$ 13 TeV with the ATLAS detector, Phys. Lett. B **754**, 302 (2016).
[59] P. Gregory, *Bayesian Logical Data Analysis for the Physical Sciences* (Cambridge University Press, Cambridge, England, 2005).
[60] ATLAS Collaboration, Luminosity determination in pp collisions at $\sqrt{s} = 8$ TeV using the ATLAS detector at the LHC, Eur. Phys. J. C **76**, 653 (2016).
[61] ATLAS Collaboration, Performance of jet substructure techniques for large-R jets in proton–proton collisions at $\sqrt{s} = 7$ TeV using the ATLAS detector, J. High Energy Phys. 09 (2013) 076.
[62] ATLAS Collaboration, Measurement of the Inelastic Proton–Proton Cross Section at $\sqrt{s} = 13$ TeV with the ATLAS Detector at the LHC, Phys. Rev. Lett. **117**, 182002 (2016).
[63] A. Buckley, J. Ferrando, S. Lloyd, K. Nordström, B. Page, M. Rüfenacht, M. Schönherr, and G. Watt, LHAPDF6: Parton density access in the LHC precision era, Eur. Phys. J. C **75**, 132 (2015).
[64] G. Cowan, K. Cranmer, E. Gross, and O. Vitells, Asymptotic formulae for likelihood-based tests of new physics, Eur. Phys. J. C **71**, 1554 (2011); Eur. Phys. J. CErratum **73**, 2501 (2013).
[65] A. L. Read, Presentation of search results: The CL_s technique, J. Phys. G **28**, 2693 (2002).
[66] T. Junk, Confidence level computation for combining searches with small statistics, Nucl. Instrum. Methods Phys. Res., Sect. A **434**, 435 (1999).
[67] C. Patrignani *et al.*, Review of particle physics, Chin. Phys. C **40**, 100001 (2016).
[68] D. de Florian *et al.*, Handbook of LHC Higgs cross sections: 4. Deciphering the nature of the Higgs sector, arXiv:1610.07922.
[69] G. Choudalakis and D. Casadei, Plotting the differences between data and expectation, Eur. Phys. J. Plus **127**, 25 (2012).
[70] ATLAS Collaboration, ATLAS computing acknowledgements, Report No. ATL-GEN-PUB-2016-002, https://cds.cern.ch/record/2202407.

M. Aaboud,[34d] G. Aad,[99] B. Abbott,[124] O. Abdinov,[13,a] B. Abeloos,[128] S. H. Abidi,[165] O. S. AbouZeid,[143] N. L. Abraham,[153] H. Abramowicz,[159] H. Abreu,[158] Y. Abulaiti,[6] B. S. Acharya,[64a,64b,b] S. Adachi,[161] L. Adamczyk,[81a] J. Adelman,[119] M. Adersberger,[112] T. Adye,[141] A. A. Affolder,[143] Y. Afik,[158] C. Agheorghiesei,[27c] J. A. Aguilar-Saavedra,[136f,136a] F. Ahmadov,[77,c] G. Aielli,[71a,71b] S. Akatsuka,[83] T. P. A. Åkesson,[94] E. Akilli,[52] A. V. Akimov,[108] G. L. Alberghi,[23b,23a] J. Albert,[174] P. Albicocco,[49] M. J. Alconada Verzini,[86] S. Alderweireldt,[117] M. Aleksa,[35] I. N. Aleksandrov,[77] C. Alexa,[27b] G. Alexander,[159] T. Alexopoulos,[10] M. Alhroob,[124] B. Ali,[138] G. Alimonti,[66a] J. Alison,[36] S. P. Alkire,[145] C. Allaire,[128] B. M. M. Allbrooke,[153] B. W. Allen,[127] P. P. Allport,[21] A. Aloisio,[67a,67b] A. Alonso,[39] F. Alonso,[86] C. Alpigiani,[145] A. A. Alshehri,[55] M. I. Alstaty,[99] B. Alvarez Gonzalez,[35] D. Álvarez Piqueras,[172] M. G. Alviggi,[67a,67b] B. T. Amadio,[18] Y. Amaral Coutinho,[78b] L. Ambroz,[131] C. Amelung,[26] D. Amidei,[103] S. P. Amor Dos Santos,[136a,136c] S. Amoroso,[35] C. S. Amrouche,[52] C. Anastopoulos,[146] L. S. Ancu,[52] N. Andari,[21] T. Andeen,[11] C. F. Anders,[59b] J. K. Anders,[20] K. J. Anderson,[36] A. Andreazza,[66a,66b] V. Andrei,[59a] S. Angelidakis,[37] I. Angelozzi,[118] A. Angerami,[38] A. V. Anisenkov,[120b,120a] A. Annovi,[69a] C. Antel,[59a] M. T. Anthony,[146] M. Antonelli,[49] D. J. A. Antrim,[169] F. Anulli,[70a] M. Aoki,[79] L. Aperio Bella,[35] G. Arabidze,[104] Y. Arai,[79] J. P. Araque,[136a] V. Araujo Ferraz,[78b] R. Araujo Pereira,[78b] A. T. H. Arce,[47] R. E. Ardell,[91] F. A. Arduh,[86] J-F. Arguin,[107] S. Argyropoulos,[75] A. J. Armbruster,[35] L. J. Armitage,[90] O. Arnaez,[165] H. Arnold,[118] M. Arratia,[31] O. Arslan,[24] A. Artamonov,[109,a] G. Artoni,[131] S. Artz,[97] S. Asai,[161] N. Asbah,[44] A. Ashkenazi,[159] E. M. Asimakopoulou,[170] L. Asquith,[153] K. Assamagan,[29] R. Astalos,[28a] R. J. Atkin,[32a] M. Atkinson,[171] N. B. Atlay,[148] K. Augsten,[138] G. Avolio,[35] R. Avramidou,[58a] B. Axen,[18] M. K. Ayoub,[15a] G. Azuelos,[107,d] A. E. Baas,[59a] M. J. Baca,[21] H. Bachacou,[142] K. Bachas,[65a,65b] M. Backes,[131] P. Bagnaia,[70a,70b] M. Bahmani,[82] H. Bahrasemani,[149] A. J. Bailey,[172] J. T. Baines,[141] M. Bajic,[39] O. K. Baker,[181] P. J. Bakker,[118] D. Bakshi Gupta,[93] E. M. Baldin,[120b,120a] P. Balek,[178] F. Balli,[142] W. K. Balunas,[133] E. Banas,[82] A. Bandyopadhyay,[24] S. Banerjee,[179,e] A. A. E. Bannoura,[180]

L. Barak,[159] W. M. Barbe,[37] E. L. Barberio,[102] D. Barberis,[53b,53a] M. Barbero,[99] T. Barillari,[113] M-S. Barisits,[35] J. Barkeloo,[127] T. Barklow,[150] N. Barlow,[31] R. Barnea,[158] S. L. Barnes,[58c] B. M. Barnett,[141] R. M. Barnett,[18] Z. Barnovska-Blenessy,[58a] A. Baroncelli,[72a] G. Barone,[26] A. J. Barr,[131] L. Barranco Navarro,[172] F. Barreiro,[96] J. Barreiro Guimarães da Costa,[15a] R. Bartoldus,[150] A. E. Barton,[87] P. Bartos,[28a] A. Basalaev,[134] A. Bassalat,[128] R. L. Bates,[55] S. J. Batista,[165] S. Batlamous,[34e] J. R. Batley,[31] M. Battaglia,[143] M. Bauce,[70a,70b] F. Bauer,[142] K. T. Bauer,[169] H. S. Bawa,[150,f] J. B. Beacham,[122] M. D. Beattie,[87] T. Beau,[132] P. H. Beauchemin,[168] P. Bechtle,[24] H. C. Beck,[51] H. P. Beck,[20,g] K. Becker,[50] M. Becker,[97] C. Becot,[121] A. Beddall,[12d] A. J. Beddall,[12a] V. A. Bednyakov,[77] M. Bedognetti,[118] C. P. Bee,[152] T. A. Beermann,[35] M. Begalli,[78b] M. Begel,[29] A. Behera,[152] J. K. Behr,[44] A. S. Bell,[92] G. Bella,[159] L. Bellagamba,[23b] A. Bellerive,[33] M. Bellomo,[158] K. Belotskiy,[110] N. L. Belyaev,[110] O. Benary,[159,a] D. Benchekroun,[34a] M. Bender,[112] N. Benekos,[10] Y. Benhammou,[159] E. Benhar Noccioli,[181] J. Benitez,[75] D. P. Benjamin,[47] M. Benoit,[52] J. R. Bensinger,[26] S. Bentvelsen,[118] L. Beresford,[131] M. Beretta,[49] D. Berge,[44] E. Bergeaas Kuutmann,[170] N. Berger,[5] L. J. Bergsten,[26] J. Beringer,[18] S. Berlendis,[56] N. R. Bernard,[100] G. Bernardi,[132] C. Bernius,[150] F. U. Bernlochner,[24] T. Berry,[91] P. Berta,[97] C. Bertella,[15a] G. Bertoli,[43a,43b] I. A. Bertram,[87] C. Bertsche,[44] G. J. Besjes,[39] O. Bessidskaia Bylund,[43a,43b] M. Bessner,[44] N. Besson,[142] A. Bethani,[98] S. Bethke,[113] A. Betti,[24] A. J. Bevan,[90] J. Beyer,[113] R. M. B. Bianchi,[135] O. Biebel,[112] D. Biedermann,[19] R. Bielski,[98] K. Bierwagen,[97] N. V. Biesuz,[69a,69b] M. Biglietti,[72a] T. R. V. Billoud,[107] M. Bindi,[51] A. Bingul,[12d] C. Bini,[70a,70b] S. Biondi,[23b,23a] T. Bisanz,[51] C. Bittrich,[46] D. M. Bjergaard,[47] J. E. Black,[150] K. M. Black,[25] R. E. Blair,[6] T. Blazek,[28a] I. Bloch,[44] C. Blocker,[26] A. Blue,[55] U. Blumenschein,[90] Dr. Blunier,[144a] G. J. Bobbink,[118] V. S. Bobrovnikov,[120b,120a] S. S. Bocchetta,[94] A. Bocci,[47] C. Bock,[112] D. Boerner,[180] D. Bogavac,[112] A. G. Bogdanchikov,[120b,120a] C. Bohm,[43a] V. Boisvert,[91] P. Bokan,[170,h] T. Bold,[81a] A. S. Boldyrev,[111] A. E. Bolz,[59b] M. Bomben,[132] M. Bona,[90] J. S. Bonilla,[127] M. Boonekamp,[142] A. Borisov,[140] G. Borissov,[87] J. Bortfeldt,[35] D. Bortoletto,[131] V. Bortolotto,[71a,61b,61c,71b] D. Boscherini,[23b] M. Bosman,[14] J. D. Bossio Sola,[30] J. Boudreau,[135] E. V. Bouhova-Thacker,[87] D. Boumediene,[37] C. Bourdarios,[128] S. K. Boutle,[55] A. Boveia,[122] J. Boyd,[35] I. R. Boyko,[77] A. J. Bozson,[91] J. Bracinik,[21] N. Brahimi,[99] A. Brandt,[8] G. Brandt,[180] O. Brandt,[59a] F. Braren,[44] U. Bratzler,[162] B. Brau,[100] J. E. Brau,[127] W. D. Breaden Madden,[55] K. Brendlinger,[44] A. J. Brennan,[102] L. Brenner,[44] R. Brenner,[170] S. Bressler,[178] B. Brickwedde,[97] D. L. Briglin,[21] T. M. Bristow,[48] D. Britton,[55] D. Britzger,[59b] I. Brock,[24] R. Brock,[104] G. Brooijmans,[38] T. Brooks,[91] W. K. Brooks,[144b] E. Brost,[119] J. H Broughton,[21] P. A. Bruckman de Renstrom,[82] D. Bruncko,[28b] A. Bruni,[23b] G. Bruni,[23b] L. S. Bruni,[118] S. Bruno,[71a,71b] B. H. Brunt,[31] M. Bruschi,[23b] N. Bruscino,[135] P. Bryant,[36] L. Bryngemark,[44] T. Buanes,[17] Q. Buat,[35] P. Buchholz,[148] A. G. Buckley,[55] I. A. Budagov,[77] F. Buehrer,[50] M. K. Bugge,[130] O. Bulekov,[110] D. Bullock,[8] T. J. Burch,[119] S. Burdin,[88] C. D. Burgard,[118] A. M. Burger,[5] B. Burghgrave,[119] K. Burka,[82] S. Burke,[141] I. Burmeister,[45] J. T. P. Burr,[131] D. Büscher,[50] V. Büscher,[97] E. Buschmann,[51] P. Bussey,[55] J. M. Butler,[25] C. M. Buttar,[55] J. M. Butterworth,[92] P. Butti,[35] W. Buttinger,[35] A. Buzatu,[155] A. R. Buzykaev,[120b,120a] G. Cabras,[23b,23a] S. Cabrera Urbán,[172] D. Caforio,[138] H. Cai,[171] V. M. M. Cairo,[2] O. Cakir,[4a] N. Calace,[52] P. Calafiura,[18] A. Calandri,[99] G. Calderini,[132] P. Calfayan,[63] G. Callea,[40b,40a] L. P. Caloba,[78b] S. Calvente Lopez,[96] D. Calvet,[37] S. Calvet,[37] T. P. Calvet,[152] M. Calvetti,[69a,69b] R. Camacho Toro,[36] S. Camarda,[35] P. Camarri,[71a,71b] D. Cameron,[130] R. Caminal Armadans,[100] C. Camincher,[56] S. Campana,[35] M. Campanelli,[92] A. Camplani,[66a,66b] A. Campoverde,[148] V. Canale,[67a,67b] M. Cano Bret,[58c] J. Cantero,[125] T. Cao,[159] Y. Cao,[171] M. D. M. Capeans Garrido,[35] I. Caprini,[27b] M. Caprini,[27b] M. Capua,[40b,40a] R. M. Carbone,[38] R. Cardarelli,[71a] F. C. Cardillo,[50] I. Carli,[139] T. Carli,[35] G. Carlino,[67a] B. T. Carlson,[135] L. Carminati,[66a,66b] R. M. D. Carney,[43a,43b] S. Caron,[117] E. Carquin,[144b] S. Carrá,[66a,66b] G. D. Carrillo-Montoya,[35] D. Casadei,[32b] M. P. Casado,[14,i] A. F. Casha,[165] M. Casolino,[14] D. W. Casper,[169] R. Castelijn,[118] V. Castillo Gimenez,[172] N. F. Castro,[136a,136e] A. Catinaccio,[35] J. R. Catmore,[130] A. Cattai,[35] J. Caudron,[24] V. Cavaliere,[29] E. Cavallaro,[14] D. Cavalli,[66a] M. Cavalli-Sforza,[14] V. Cavasinni,[69a,69b] E. Celebi,[12b] F. Ceradini,[72a,72b] L. Cerda Alberich,[172] A. S. Cerqueira,[78a] A. Cerri,[153] L. Cerrito,[71a,71b] F. Cerutti,[18] A. Cervelli,[23b,23a] S. A. Cetin,[12b] A. Chafaq,[34a] D Chakraborty,[119] S. K. Chan,[57] W. S. Chan,[118] Y. L. Chan,[61a] P. Chang,[171] J. D. Chapman,[31] D. G. Charlton,[21] C. C. Chau,[33] C. A. Chavez Barajas,[153] S. Che,[122] A. Chegwidden,[104] S. Chekanov,[6] S. V. Chekulaev,[166a] G. A. Chelkov,[77,j] M. A. Chelstowska,[35] C. Chen,[58a] C. H. Chen,[76] H. Chen,[29] J. Chen,[58a] J. Chen,[38] S. Chen,[133] S. J. Chen,[15c] X. Chen,[15b,k] Y. Chen,[80] Y-H. Chen,[44] H. C. Cheng,[103] H. J. Cheng,[15d] A. Cheplakov,[77] E. Cheremushkina,[140] R. Cherkaoui El Moursli,[34e] E. Cheu,[7] K. Cheung,[62] L. Chevalier,[142] V. Chiarella,[49] G. Chiarelli,[69a] G. Chiodini,[65a] A. S. Chisholm,[35] A. Chitan,[27b] I. Chiu,[161] Y. H. Chiu,[174] M. V. Chizhov,[77] K. Choi,[63] A. R. Chomont,[128] S. Chouridou,[160] Y. S. Chow,[118] V. Christodoulou,[92] M. C. Chu,[61a] J. Chudoba,[137] A. J. Chuinard,[101] J. J. Chwastowski,[82] L. Chytka,[126] D. Cinca,[45] V. Cindro,[89] I. A. Cioară,[24] A. Ciocio,[18] F. Cirotto,[67a,67b] Z. H. Citron,[178] M. Citterio,[66a] A. Clark,[52]

M. R. Clark,[38] P. J. Clark,[48] R. N. Clarke,[18] C. Clement,[43a,43b] Y. Coadou,[99] M. Cobal,[64a,64c] A. Coccaro,[53b,53a] J. Cochran,[76] A. E. C. Coimbra,[178] L. Colasurdo,[117] B. Cole,[38] A. P. Colijn,[118] J. Collot,[56] P. Conde Muiño,[136a,136b] E. Coniavitis,[50] S. H. Connell,[32b] I. A. Connelly,[98] S. Constantinescu,[27b] F. Conventi,[67a,l] A. M. Cooper-Sarkar,[131] F. Cormier,[173] K. J. R. Cormier,[165] M. Corradi,[70a,70b] E. E. Corrigan,[94] F. Corriveau,[101,m] A. Cortes-Gonzalez,[35] M. J. Costa,[172] D. Costanzo,[146] G. Cottin,[31] G. Cowan,[91] B. E. Cox,[98] J. Crane,[98] K. Cranmer,[121] S. J. Crawley,[55] R. A. Creager,[133] G. Cree,[33] S. Crépé-Renaudin,[56] F. Crescioli,[132] M. Cristinziani,[24] V. Croft,[121] G. Crosetti,[40b,40a] A. Cueto,[96] T. Cuhadar Donszelmann,[146] A. R. Cukierman,[150] M. Curatolo,[49] J. Cúth,[97] S. Czekierda,[82] P. Czodrowski,[35] M. J. Da Cunha Sargedas De Sousa,[58b,136b] C. Da Via,[98] W. Dabrowski,[81a] T. Dado,[28a,h] S. Dahbi,[34e] T. Dai,[103] O. Dale,[17] F. Dallaire,[107] C. Dallapiccola,[100] M. Dam,[39] G. D'amen,[23b,23a] J. R. Dandoy,[133] M. F. Daneri,[30] N. P. Dang,[179,e] N. D Dann,[98] M. Danninger,[173] V. Dao,[35] G. Darbo,[53b] S. Darmora,[8] O. Dartsi,[5] A. Dattagupta,[127] T. Daubney,[44] S. D'Auria,[55] W. Davey,[24] C. David,[44] T. Davidek,[139] D. R. Davis,[47] E. Dawe,[102] I. Dawson,[146] K. De,[8] R. De Asmundis,[67a] A. De Benedetti,[124] S. De Castro,[23b,23a] S. De Cecco,[132] N. De Groot,[117] P. de Jong,[118] H. De la Torre,[104] F. De Lorenzi,[76] A. De Maria,[51,n] D. De Pedis,[70a] A. De Salvo,[70a] U. De Sanctis,[71a,71b] A. De Santo,[153] K. De Vasconcelos Corga,[99] J. B. De Vivie De Regie,[128] C. Debenedetti,[143] D. V. Dedovich,[77] N. Dehghanian,[3] M. Del Gaudio,[40b,40a] J. Del Peso,[96] D. Delgove,[128] F. Deliot,[142] C. M. Delitzsch,[7] M. Della Pietra,[67a,67b] D. Della Volpe,[52] A. Dell'Acqua,[35] L. Dell'Asta,[25] M. Delmastro,[5] C. Delporte,[128] P. A. Delsart,[56] D. A. DeMarco,[165] S. Demers,[181] M. Demichev,[77] S. P. Denisov,[140] D. Denysiuk,[118] L. D'Eramo,[132] D. Derendarz,[82] J. E. Derkaoui,[34d] F. Derue,[132] P. Dervan,[88] K. Desch,[24] C. Deterre,[44] K. Dette,[165] M. R. Devesa,[30] P. O. Deviveiros,[35] A. Dewhurst,[141] S. Dhaliwal,[26] F. A. Di Bello,[52] A. Di Ciaccio,[71a,71b] L. Di Ciaccio,[5] W. K. Di Clemente,[133] C. Di Donato,[67a,67b] A. Di Girolamo,[35] B. Di Micco,[72a,72b] R. Di Nardo,[35] K. F. Di Petrillo,[57] A. Di Simone,[50] R. Di Sipio,[165] D. Di Valentino,[33] C. Diaconu,[99] M. Diamond,[165] F. A. Dias,[39] T. Dias Do Vale,[136a] M. A. Diaz,[144a] J. Dickinson,[18] E. B. Diehl,[103] J. Dietrich,[19] S. Díez Cornell,[44] A. Dimitrievska,[18] J. Dingfelder,[24] F. Dittus,[35] F. Djama,[99] T. Djobava,[157b] J. I. Djuvsland,[59a] M. A. B. Do Vale,[78c] M. Dobre,[27b] D. Dodsworth,[26] C. Doglioni,[94] J. Dolejsi,[139] Z. Dolezal,[139] M. Donadelli,[78d] J. Donini,[37] A. D'onofrio,[90] M. D'Onofrio,[88] J. Dopke,[141] A. Doria,[67a] M. T. Dova,[86] A. T. Doyle,[55] E. Drechsler,[51] E. Dreyer,[149] T. Dreyer,[51] M. Dris,[10] Y. Du,[58b] J. Duarte-Campderros,[159] F. Dubinin,[108] A. Dubreuil,[52] E. Duchovni,[178] G. Duckeck,[112] A. Ducourthial,[132] O. A. Ducu,[107,o] D. Duda,[118] A. Dudarev,[35] A. C. Dudder,[97] E. M. Duffield,[18] L. Duflot,[128] M. Dührssen,[35] C. Dülsen,[180] M. Dumancic,[178] A. E. Dumitriu,[27b,p] A. K. Duncan,[55] M. Dunford,[59a] A. Duperrin,[99] H. Duran Yildiz,[4a] M. Düren,[54] A. Durglishvili,[157b] D. Duschinger,[46] B. Dutta,[44] D. Duvnjak,[1] M. Dyndal,[44] B. S. Dziedzic,[82] C. Eckardt,[44] K. M. Ecker,[113] R. C. Edgar,[103] T. Eifert,[35] G. Eigen,[17] K. Einsweiler,[18] T. Ekelof,[170] M. El Kacimi,[34c] R. El Kosseifi,[99] V. Ellajosyula,[99] M. Ellert,[170] F. Ellinghaus,[180] A. A. Elliot,[174] N. Ellis,[35] J. Elmsheuser,[29] M. Elsing,[35] D. Emeliyanov,[141] Y. Enari,[161] J. S. Ennis,[176] M. B. Epland,[47] J. Erdmann,[45] A. Ereditato,[20] S. Errede,[171] M. Escalier,[128] C. Escobar,[172] B. Esposito,[49] O. Estrada Pastor,[172] A. I. Etienvre,[142] E. Etzion,[159] H. Evans,[63] A. Ezhilov,[134] M. Ezzi,[34e] F. Fabbri,[23b,23a] L. Fabbri,[23b,23a] V. Fabiani,[117] G. Facini,[92] R. M. Faisca Rodrigues Pereira,[136a] R. M. Fakhrutdinov,[140] S. Falciano,[70a] P. J. Falke,[5] S. Falke,[5] J. Faltova,[139] Y. Fang,[15a] M. Fanti,[66a,66b] A. Farbin,[8] A. Farilla,[72a] E. M. Farina,[68a,68b] T. Farooque,[104] S. Farrell,[18] S. M. Farrington,[176] P. Farthouat,[35] F. Fassi,[34e] P. Fassnacht,[35] D. Fassouliotis,[9] M. Faucci Giannelli,[48] A. Favareto,[53b,53a] W. J. Fawcett,[52] L. Fayard,[128] O. L. Fedin,[134,q] W. Fedorko,[173] M. Feickert,[41] S. Feigl,[130] L. Feligioni,[99] C. Feng,[58b] E. J. Feng,[35] M. Feng,[47] M. J. Fenton,[55] A. B. Fenyuk,[140] L. Feremenga,[8] J. Ferrando,[44] A. Ferrari,[170] P. Ferrari,[118] R. Ferrari,[68a] D. E. Ferreira de Lima,[59b] A. Ferrer,[172] D. Ferrere,[52] C. Ferretti,[103] F. Fiedler,[97] A. Filipčič,[89] F. Filthaut,[117] M. Fincke-Keeler,[174] K. D. Finelli,[25] M. C. N. Fiolhais,[136a,136c,r] L. Fiorini,[172] C. Fischer,[14] J. Fischer,[180] W. C. Fisher,[104] N. Flaschel,[44] I. Fleck,[148] P. Fleischmann,[103] R. R. M. Fletcher,[133] T. Flick,[180] B. M. Flierl,[112] L. M. Flores,[133] L. R. Flores Castillo,[61a] N. Fomin,[17] G. T. Forcolin,[98] A. Formica,[142] F. A. Förster,[14] A. C. Forti,[98] A. G. Foster,[21] D. Fournier,[128] H. Fox,[87] S. Fracchia,[146] P. Francavilla,[69a,69b] M. Franchini,[23b,23a] S. Franchino,[59a] D. Francis,[35] L. Franconi,[130] M. Franklin,[57] M. Frate,[169] M. Fraternali,[68a,68b] D. Freeborn,[92] S. M. Fressard-Batraneanu,[35] B. Freund,[107] W. S. Freund,[78b] D. Froidevaux,[35] J. A. Frost,[131] C. Fukunaga,[162] T. Fusayasu,[114] J. Fuster,[172] O. Gabizon,[158] A. Gabrielli,[23b,23a] A. Gabrielli,[18] G. P. Gach,[81a] S. Gadatsch,[52] S. Gadomski,[52] P. Gadow,[113] G. Gagliardi,[53b,53a] L. G. Gagnon,[107] C. Galea,[27b] B. Galhardo,[136a,136c] E. J. Gallas,[131] B. J. Gallop,[141] P. Gallus,[138] G. Galster,[39] R. Gamboa Goni,[90] K. K. Gan,[122] S. Ganguly,[178] Y. Gao,[88] Y. S. Gao,[150,f] C. García,[172] J. E. García Navarro,[172] J. A. García Pascual,[15a] M. Garcia-Sciveres,[18] R. W. Gardner,[36] N. Garelli,[150] V. Garonne,[130] K. Gasnikova,[44] A. Gaudiello,[53b,53a] G. Gaudio,[68a] I. L. Gavrilenko,[108] A. Gavrilyuk,[109] C. Gay,[173] G. Gaycken,[24] E. N. Gazis,[10]

C. N. P. Gee,[141] J. Geisen,[51] M. Geisen,[97] M. P. Geisler,[59a] K. Gellerstedt,[43a,43b] C. Gemme,[53b] M. H. Genest,[56] C. Geng,[103] S. Gentile,[70a,70b] C. Gentsos,[160] S. George,[91] D. Gerbaudo,[14] G. Gessner,[45] S. Ghasemi,[148] M. Ghneimat,[24] B. Giacobbe,[23b] S. Giagu,[70a,70b] N. Giangiacomi,[23b,23a] P. Giannetti,[69a] S. M. Gibson,[91] M. Gignac,[143] D. Gillberg,[33] G. Gilles,[180] D. M. Gingrich,[3,d] M. P. Giordani,[64a,64c] F. M. Giorgi,[23b] P. F. Giraud,[142] P. Giromini,[57] G. Giugliarelli,[64a,64c] D. Giugni,[66a] F. Giuli,[131] M. Giulini,[59b] S. Gkaitatzis,[160] I. Gkialas,[9,s] E. L. Gkougkousis,[14] P. Gkountoumis,[10] L. K. Gladilin,[111] C. Glasman,[96] J. Glatzer,[14] P. C. F. Glaysher,[44] A. Glazov,[44] M. Goblirsch-Kolb,[26] J. Godlewski,[82] S. Goldfarb,[102] T. Golling,[52] D. Golubkov,[140] A. Gomes,[136a,136b,136d] R. Goncalves Gama,[78a] R. Gonçalo,[136a] G. Gonella,[50] L. Gonella,[21] A. Gongadze,[77] F. Gonnella,[21] J. L. Gonski,[57] S. González de la Hoz,[172] S. Gonzalez-Sevilla,[52] L. Goossens,[35] P. A. Gorbounov,[109] H. A. Gordon,[29] B. Gorini,[35] E. Gorini,[65a,65b] A. Gorišek,[89] A. T. Goshaw,[47] C. Gössling,[45] M. I. Gostkin,[77] C. A. Gottardo,[24] C. R. Goudet,[128] D. Goujdami,[34c] A. G. Goussiou,[145] N. Govender,[32b,t] C. Goy,[5] E. Gozani,[158] I. Grabowska-Bold,[81a] P. O. J. Gradin,[170] E. C. Graham,[88] J. Gramling,[169] E. Gramstad,[130] S. Grancagnolo,[19] V. Gratchev,[134] P. M. Gravila,[27f] C. Gray,[55] H. M. Gray,[18] Z. D. Greenwood,[93,u] C. Grefe,[24] K. Gregersen,[92] I. M. Gregor,[44] P. Grenier,[150] K. Grevtsov,[44] J. Griffiths,[8] A. A. Grillo,[143] K. Grimm,[150] S. Grinstein,[14,v] Ph. Gris,[37] J.-F. Grivaz,[128] S. Groh,[97] E. Gross,[178] J. Grosse-Knetter,[51] G. C. Grossi,[93] Z. J. Grout,[92] A. Grummer,[116] L. Guan,[103] W. Guan,[179] J. Guenther,[35] A. Guerguichon,[128] F. Guescini,[166a] D. Guest,[169] O. Gueta,[159] R. Gugel,[50] B. Gui,[122] T. Guillemin,[5] S. Guindon,[35] U. Gul,[55] C. Gumpert,[35] J. Guo,[58c] W. Guo,[103] Y. Guo,[58a,w] Z. Guo,[99] R. Gupta,[41] S. Gurbuz,[12c] G. Gustavino,[124] B. J. Gutelman,[158] P. Gutierrez,[124] N. G. Gutierrez Ortiz,[92] C. Gutschow,[92] C. Guyot,[142] M. P. Guzik,[81a] C. Gwenlan,[131] C. B. Gwilliam,[88] A. Haas,[121] C. Haber,[18] H. K. Hadavand,[8] N. Haddad,[34e] A. Hadef,[99] S. Hageböck,[24] M. Hagihara,[167] H. Hakobyan,[182,a] M. Haleem,[175] J. Haley,[125] G. Halladjian,[104] G. D. Hallewell,[99] K. Hamacher,[180] P. Hamal,[126] K. Hamano,[174] A. Hamilton,[32a] G. N. Hamity,[146] K. Han,[58a,x] L. Han,[58a] S. Han,[15d] K. Hanagaki,[79,y] M. Hance,[143] D. M. Handl,[112] B. Haney,[133] R. Hankache,[132] P. Hanke,[59a] E. Hansen,[94] J. B. Hansen,[39] J. D. Hansen,[39] M. C. Hansen,[24] P. H. Hansen,[39] K. Hara,[167] A. S. Hard,[179] T. Harenberg,[180] S. Harkusha,[105] P. F. Harrison,[176] N. M. Hartmann,[112] Y. Hasegawa,[147] A. Hasib,[48] S. Hassani,[142] S. Haug,[20] R. Hauser,[104] L. Hauswald,[46] L. B. Havener,[38] M. Havranek,[138] C. M. Hawkes,[21] R. J. Hawkings,[35] D. Hayden,[104] C. Hayes,[152] C. P. Hays,[131] J. M. Hays,[90] H. S. Hayward,[88] S. J. Haywood,[141] M. P. Heath,[48] V. Hedberg,[94] L. Heelan,[8] S. Heer,[24] K. K. Heidegger,[50] J. Heilman,[33] S. Heim,[44] T. Heim,[18] B. Heinemann,[44,z] J. J. Heinrich,[112] L. Heinrich,[121] C. Heinz,[54] J. Hejbal,[137] L. Helary,[35] A. Held,[173] S. Hellesund,[130] S. Hellman,[43a,43b] C. Helsens,[35] R. C. W. Henderson,[87] Y. Heng,[179] S. Henkelmann,[173] A. M. Henriques Correia,[35] G. H. Herbert,[19] H. Herde,[26] V. Herget,[175] Y. Hernández Jiménez,[32c] H. Herr,[97] G. Herten,[50] R. Hertenberger,[112] L. Hervas,[35] T. C. Herwig,[133] G. G. Hesketh,[92] N. P. Hessey,[166a] J. W. Hetherly,[41] S. Higashino,[79] E. Higón-Rodriguez,[172] K. Hildebrand,[36] E. Hill,[174] J. C. Hill,[31] K. H. Hiller,[44] S. J. Hillier,[21] M. Hils,[46] I. Hinchliffe,[18] M. Hirose,[129] D. Hirschbuehl,[180] B. Hiti,[89] O. Hladik,[137] D. R. Hlaluku,[32c] X. Hoad,[48] J. Hobbs,[152] N. Hod,[166a] M. C. Hodgkinson,[146] A. Hoecker,[35] M. R. Hoeferkamp,[116] F. Hoenig,[112] D. Hohn,[24] D. Hohov,[128] T. R. Holmes,[36] M. Holzbock,[112] M. Homann,[45] S. Honda,[167] T. Honda,[79] T. M. Hong,[135] A. Hönle,[113] B. H. Hooberman,[171] W. H. Hopkins,[127] Y. Horii,[115] P. Horn,[46] A. J. Horton,[149] L. A. Horyn,[36] J-Y. Hostachy,[56] A. Hostiuc,[145] S. Hou,[155] A. Hoummada,[34a] J. Howarth,[98] J. Hoya,[86] M. Hrabovsky,[126] J. Hrdinka,[35] I. Hristova,[19] J. Hrivnac,[128] A. Hrynevich,[106] T. Hryn'ova,[5] P. J. Hsu,[62] S.-C. Hsu,[145] Q. Hu,[29] S. Hu,[58c] Y. Huang,[15a] Z. Hubacek,[138] F. Hubaut,[99] M. Huebner,[24] F. Huegging,[24] T. B. Huffman,[131] E. W. Hughes,[38] M. Huhtinen,[35] R. F. H. Hunter,[33] P. Huo,[152] A. M. Hupe,[33] N. Huseynov,[77,c] J. Huston,[104] J. Huth,[57] R. Hyneman,[103] G. Iacobucci,[52] G. Iakovidis,[29] I. Ibragimov,[148] L. Iconomidou-Fayard,[128] Z. Idrissi,[34e] P. Iengo,[35] R. Ignazzi,[39] O. Igonkina,[118,aa] R. Iguchi,[161] T. Iizawa,[177] Y. Ikegami,[79] M. Ikeno,[79] D. Iliadis,[160] N. Ilic,[150] F. Iltzsche,[46] G. Introzzi,[68a,68b] M. Iodice,[72a] K. Iordanidou,[38] V. Ippolito,[70a,70b] M. F. Isacson,[170] N. Ishijima,[129] M. Ishino,[161] M. Ishitsuka,[163] C. Issever,[131] S. Istin,[12c,bb] F. Ito,[167] J. M. Iturbe Ponce,[61a] R. Iuppa,[73a,73b] A. Ivina,[178] H. Iwasaki,[79] J. M. Izen,[42] V. Izzo,[67a] S. Jabbar,[3] P. Jacka,[137] P. Jackson,[1] R. M. Jacobs,[24] V. Jain,[2] G. Jäkel,[180] K. B. Jakobi,[97] K. Jakobs,[50] S. Jakobsen,[74] T. Jakoubek,[137] D. O. Jamin,[125] D. K. Jana,[93] R. Jansky,[52] J. Janssen,[24] M. Janus,[51] P. A. Janus,[81a] G. Jarlskog,[94] N. Javadov,[77,c] T. Javůrek,[50] M. Javurkova,[50] F. Jeanneau,[142] L. Jeanty,[18] J. Jejelava,[157a,cc] A. Jelinskas,[176] P. Jenni,[50,dd] J. Jeong,[44] C. Jeske,[176] S. Jézéquel,[5] H. Ji,[179] J. Jia,[152] H. Jiang,[76] Y. Jiang,[58a] Z. Jiang,[150] S. Jiggins,[50] F. A. Jimenez Morales,[37] J. Jimenez Pena,[172] S. Jin,[15c] A. Jinaru,[27b] O. Jinnouchi,[163] H. Jivan,[32c] P. Johansson,[146] K. A. Johns,[7] C. A. Johnson,[63] W. J. Johnson,[145] K. Jon-And,[43a,43b] R. W. L. Jones,[87] S. D. Jones,[153] S. Jones,[7] T. J. Jones,[88] J. Jongmanns,[59a] P. M. Jorge,[136a,136b] J. Jovicevic,[166a] X. Ju,[179] J. J. Junggeburth,[113] A. Juste Rozas,[14,v] A. Kaczmarska,[82] M. Kado,[128] H. Kagan,[122] M. Kagan,[150] T. Kaji,[177] E. Kajomovitz,[158] C. W. Kalderon,[94] A. Kaluza,[97] S. Kama,[41] A. Kamenshchikov,[140] L. Kanjir,[89] Y. Kano,[161]

V. A. Kantserov,[110] J. Kanzaki,[79] B. Kaplan,[121] L. S. Kaplan,[179] D. Kar,[32c] M. J. Kareem,[166b] E. Karentzos,[10] S. N. Karpov,[77] Z. M. Karpova,[77] V. Kartvelishvili,[87] A. N. Karyukhin,[140] K. Kasahara,[167] L. Kashif,[179] R. D. Kass,[122] A. Kastanas,[151] Y. Kataoka,[161] C. Kato,[161] A. Katre,[52] J. Katzy,[44] K. Kawade,[80] K. Kawagoe,[85] T. Kawamoto,[161] G. Kawamura,[51] E. F. Kay,[88] V. F. Kazanin,[120b,120a] R. Keeler,[174] R. Kehoe,[41] J. S. Keller,[33] E. Kellermann,[94] J. J. Kempster,[21] J. Kendrick,[21] O. Kepka,[137] S. Kersten,[180] B. P. Kerševan,[89] R. A. Keyes,[101] M. Khader,[171] F. Khalil-Zada,[13] A. Khanov,[125] A. G. Kharlamov,[120b,120a] T. Kharlamova,[120b,120a] A. Khodinov,[164] T. J. Khoo,[52] V. Khovanskiy,[109,a] E. Khramov,[77] J. Khubua,[157b] S. Kido,[80] M. Kiehn,[52] C. R. Kilby,[91] H. Y. Kim,[8] S. H. Kim,[167] Y. K. Kim,[36] N. Kimura,[64a,64c] O. M. Kind,[19] B. T. King,[88] D. Kirchmeier,[46] J. Kirk,[141] A. E. Kiryunin,[113] T. Kishimoto,[161] D. Kisielewska,[81a] V. Kitali,[44] O. Kivernyk,[5] E. Kladiva,[28b] T. Klapdor-Kleingrothaus,[50] M. H. Klein,[103] M. Klein,[88] U. Klein,[88] K. Kleinknecht,[97] P. Klimek,[119] A. Klimentov,[29] R. Klingenberg,[45,a] T. Klingl,[24] T. Klioutchnikova,[35] F. F. Klitzner,[112] P. Kluit,[118] S. Kluth,[113] E. Kneringer,[74] E. B. F. G. Knoops,[99] A. Knue,[50] A. Kobayashi,[161] D. Kobayashi,[85] T. Kobayashi,[161] M. Kobel,[46] M. Kocian,[150] P. Kodys,[139] T. Koffas,[33] E. Koffeman,[118] N. M. Köhler,[113] T. Koi,[150] M. Kolb,[59b] I. Koletsou,[5] T. Kondo,[79] N. Kondrashova,[58c] K. Köneke,[50] A. C. König,[117] T. Kono,[79,ee] R. Konoplich,[121,ff] N. Konstantinidis,[92] B. Konya,[94] R. Kopeliansky,[63] S. Koperny,[81a] K. Korcyl,[82] K. Kordas,[160] A. Korn,[92] I. Korolkov,[14] E. V. Korolkova,[146] O. Kortner,[113] S. Kortner,[113] T. Kosek,[139] V. V. Kostyukhin,[24] A. Kotwal,[47] A. Koulouris,[10] A. Kourkoumeli-Charalampidi,[68a,68b] C. Kourkoumelis,[9] E. Kourlitis,[146] V. Kouskoura,[29] A. B. Kowalewska,[82] R. Kowalewski,[174] T. Z. Kowalski,[81a] C. Kozakai,[161] W. Kozanecki,[142] A. S. Kozhin,[140] V. A. Kramarenko,[111] G. Kramberger,[89] D. Krasnopevtsev,[110] M. W. Krasny,[132] A. Krasznahorkay,[35] D. Krauss,[113] J. A. Kremer,[81a] J. Kretzschmar,[88] K. Kreutzfeldt,[54] P. Krieger,[165] K. Krizka,[18] K. Kroeninger,[45] H. Kroha,[113] J. Kroll,[137] J. Kroll,[133] J. Kroseberg,[24] J. Krstic,[16] U. Kruchonak,[77] H. Krüger,[24] N. Krumnack,[76] M. C. Kruse,[47] T. Kubota,[102] S. Kuday,[4b] J. T. Kuechler,[180] S. Kuehn,[35] A. Kugel,[59a] F. Kuger,[175] T. Kuhl,[44] V. Kukhtin,[77] R. Kukla,[99] Y. Kulchitsky,[105] S. Kuleshov,[144b] Y. P. Kulinich,[171] M. Kuna,[56] T. Kunigo,[83] A. Kupco,[137] T. Kupfer,[45] O. Kuprash,[159] H. Kurashige,[80] L. L. Kurchaninov,[166a] Y. A. Kurochkin,[105] M. G. Kurth,[15d] E. S. Kuwertz,[174] M. Kuze,[163] J. Kvita,[126] T. Kwan,[174] A. La Rosa,[113] J. L. La Rosa Navarro,[78d] L. La Rotonda,[40b,40a] F. La Ruffa,[40b,40a] C. Lacasta,[172] F. Lacava,[70a,70b] J. Lacey,[44] D. P. J. Lack,[98] H. Lacker,[19] D. Lacour,[132] E. Ladygin,[77] R. Lafaye,[5] B. Laforge,[132] S. Lai,[51] S. Lammers,[63] W. Lampl,[7] E. Lançon,[29] U. Landgraf,[50] M. P. J. Landon,[90] M. C. Lanfermann,[52] V. S. Lang,[44] J. C. Lange,[14] R. J. Langenberg,[35] A. J. Lankford,[169] F. Lanni,[29] K. Lantzsch,[24] A. Lanza,[68a] A. Lapertosa,[53b,53a] S. Laplace,[132] J. F. Laporte,[142] T. Lari,[66a] F. Lasagni Manghi,[23b,23a] M. Lassnig,[35] T. S. Lau,[61a] A. Laudrain,[128] A. T. Law,[143] P. Laycock,[88] M. Lazzaroni,[66a,66b] B. Le,[102] O. Le Dortz,[132] E. Le Guirriec,[99] E. P. Le Quilleuc,[142] M. LeBlanc,[7] T. LeCompte,[6] F. Ledroit-Guillon,[56] C. A. Lee,[29] G. R. Lee,[144a] L. Lee,[57] S. C. Lee,[155] B. Lefebvre,[101] M. Lefebvre,[174] F. Legger,[112] C. Leggett,[18] G. Lehmann Miotto,[35] W. A. Leight,[44] A. Leisos,[160,gg] M. A. L. Leite,[78d] R. Leitner,[139] D. Lellouch,[178] B. Lemmer,[51] K. J. C. Leney,[92] T. Lenz,[24] B. Lenzi,[35] R. Leone,[7] S. Leone,[69a] C. Leonidopoulos,[48] G. Lerner,[153] C. Leroy,[107] R. Les,[165] A. A. J. Lesage,[142] C. G. Lester,[31] M. Levchenko,[134] J. Levêque,[5] D. Levin,[103] L. J. Levinson,[178] D. Lewis,[90] B. Li,[58a,w] C-Q. Li,[58a] H. Li,[58b] L. Li,[58c] Q. Li,[15d] Q. Y. Li,[58a] S. Li,[58d,58c] X. Li,[58c] Y. Li,[148] Z. Liang,[15a] B. Liberti,[71a] A. Liblong,[165] K. Lie,[61c] S. Liem,[118] A. Limosani,[154] C. Y. Lin,[31] K. Lin,[104] S. C. Lin,[156] T. H. Lin,[97] R. A. Linck,[63] B. E. Lindquist,[152] A. L. Lionti,[52] E. Lipeles,[133] A. Lipniacka,[17] M. Lisovyi,[59b] T. M. Liss,[171,hh] A. Lister,[173] A. M. Litke,[143] J. D. Little,[8] B. Liu,[76] B. L Liu,[6] H. B. Liu,[29] H. Liu,[103] J. B. Liu,[58a] J. K. K. Liu,[131] K. Liu,[132] M. Liu,[58a] P. Liu,[18] Y. L. Liu,[58a] Y. W. Liu,[58a] M. Livan,[68a,68b] A. Lleres,[56] J. Llorente Merino,[15a] S. L. Lloyd,[90] C. Y. Lo,[61b] F. Lo Sterzo,[41] E. M. Lobodzinska,[44] P. Loch,[7] F. K. Loebinger,[98] A. Loesle,[50] K. M. Loew,[26] T. Lohse,[19] K. Lohwasser,[146] M. Lokajicek,[137] B. A. Long,[25] J. D. Long,[171] R. E. Long,[87] L. Longo,[65a,65b] K. A. Looper,[122] J. A. Lopez,[144b] I. Lopez Paz,[14] A. Lopez Solis,[132] J. Lorenz,[112] N. Lorenzo Martinez,[5] M. Losada,[22] P. J. Lösel,[112] X. Lou,[44] X. Lou,[15a] A. Lounis,[128] J. Love,[6] P. A. Love,[87] J. J. Lozano Bahilo,[172] H. Lu,[61a] N. Lu,[103] Y. J. Lu,[62] H. J. Lubatti,[145] C. Luci,[70a,70b] A. Lucotte,[56] C. Luedtke,[50] F. Luehring,[63] I. Luise,[132] W. Lukas,[74] L. Luminari,[70a] B. Lund-Jensen,[151] M. S. Lutz,[100] P. M. Luzi,[132] D. Lynn,[29] R. Lysak,[137] E. Lytken,[94] F. Lyu,[15a] V. Lyubushkin,[77] H. Ma,[29] L. L. Ma,[58b] Y. Ma,[58b] G. Maccarrone,[49] A. Macchiolo,[113] C. M. Macdonald,[146] J. Machado Miguens,[133,136b] D. Madaffari,[172] R. Madar,[37] W. F. Mader,[46] A. Madsen,[44] N. Madysa,[46] J. Maeda,[80] S. Maeland,[17] T. Maeno,[29] A. S. Maevskiy,[111] V. Magerl,[50] C. Maidantchik,[78b] T. Maier,[112] A. Maio,[136a,136b,136d] O. Majersky,[28a] S. Majewski,[127] Y. Makida,[79] N. Makovec,[128] B. Malaescu,[132] Pa. Malecki,[82] V. P. Maleev,[134] F. Malek,[56] U. Mallik,[75] D. Malon,[6] C. Malone,[31] S. Maltezos,[10] S. Malyukov,[35] J. Mamuzic,[172] G. Mancini,[49] I. Mandić,[89] J. Maneira,[136a] L. Manhaes de Andrade Filho,[78a] J. Manjarres Ramos,[46] K. H. Mankinen,[94] A. Mann,[112] A. Manousos,[74] B. Mansoulie,[142] J. D. Mansour,[15a] R. Mantifel,[101] M. Mantoani,[51]

S. Manzoni,[66a,66b] G. Marceca,[30] L. March,[52] L. Marchese,[131] G. Marchiori,[132] M. Marcisovsky,[137] C. A. Marin Tobon,[35] M. Marjanovic,[37] D. E. Marley,[103] F. Marroquim,[78b] Z. Marshall,[18] M. U. F. Martensson,[170] S. Marti-Garcia,[172] C. B. Martin,[122] T. A. Martin,[176] V. J. Martin,[48] B. Martin dit Latour,[17] M. Martinez,[14,v] V. I. Martinez Outschoorn,[100] S. Martin-Haugh,[141] V. S. Martoiu,[27b] A. C. Martyniuk,[92] A. Marzin,[35] L. Masetti,[97] T. Mashimo,[161] R. Mashinistov,[108] J. Masik,[98] A. L. Maslennikov,[120b,120a] L. H. Mason,[102] L. Massa,[71a,71b] P. Mastrandrea,[5] A. Mastroberardino,[40b,40a] T. Masubuchi,[161] P. Mättig,[180] J. Maurer,[27b] B. Maček,[89] S. J. Maxfield,[88] D. A. Maximov,[120b,120a] R. Mazini,[155] I. Maznas,[160] S. M. Mazza,[143] N. C. Mc Fadden,[116] G. Mc Goldrick,[165] S. P. Mc Kee,[103] A. McCarn,[103] T. G. McCarthy,[113] L. I. McClymont,[92] E. F. McDonald,[102] J. A. Mcfayden,[35] G. Mchedlidze,[51] M. A. McKay,[41] K. D. McLean,[174] S. J. McMahon,[141] P. C. McNamara,[102] C. J. McNicol,[176] R. A. McPherson,[174,m] J. E. Mdhluli,[32c] Z. A. Meadows,[100] S. Meehan,[145] T. Megy,[50] S. Mehlhase,[112] A. Mehta,[88] T. Meideck,[56] B. Meirose,[42] D. Melini,[172,ii] B. R. Mellado Garcia,[32c] J. D. Mellenthin,[51] M. Melo,[28a] F. Meloni,[20] A. Melzer,[24] S. B. Menary,[98] L. Meng,[88] X. T. Meng,[103] A. Mengarelli,[23b,23a] S. Menke,[113] E. Meoni,[40b,40a] S. Mergelmeyer,[19] C. Merlassino,[20] P. Mermod,[52] L. Merola,[67a,67b] C. Meroni,[66a] F. S. Merritt,[36] A. Messina,[70a,70b] J. Metcalfe,[6] A. S. Mete,[169] C. Meyer,[133] J. Meyer,[158] J-P. Meyer,[142] H. Meyer Zu Theenhausen,[59a] F. Miano,[153] R. P. Middleton,[141] L. Mijović,[48] G. Mikenberg,[178] M. Mikestikova,[137] M. Mikuž,[89] M. Milesi,[102] A. Milic,[165] D. A. Millar,[90] D. W. Miller,[36] A. Milov,[178] D. A. Milstead,[43a,43b] A. A. Minaenko,[140] I. A. Minashvili,[157b] A. I. Mincer,[121] B. Mindur,[81a] M. Mineev,[77] Y. Minegishi,[161] Y. Ming,[179] L. M. Mir,[14] A. Mirto,[65a,65b] K. P. Mistry,[133] T. Mitani,[177] J. Mitrevski,[112] V. A. Mitsou,[172] A. Miucci,[20] P. S. Miyagawa,[146] A. Mizukami,[79] J. U. Mjörnmark,[94] T. Mkrtchyan,[182] M. Mlynarikova,[139] T. Moa,[43a,43b] K. Mochizuki,[107] P. Mogg,[50] S. Mohapatra,[38] S. Molander,[43a,43b] R. Moles-Valls,[24] M. C. Mondragon,[104] K. Mönig,[44] J. Monk,[39] E. Monnier,[99] A. Montalbano,[149] J. Montejo Berlingen,[35] F. Monticelli,[86] S. Monzani,[66a] R. W. Moore,[3] N. Morange,[128] D. Moreno,[22] M. Moreno Llácer,[35] P. Morettini,[53b] M. Morgenstern,[118] S. Morgenstern,[35] D. Mori,[149] T. Mori,[161] M. Morii,[57] M. Morinaga,[177] V. Morisbak,[130] A. K. Morley,[35] G. Mornacchi,[35] J. D. Morris,[90] L. Morvaj,[152] P. Moschovakos,[10] M. Mosidze,[157b] H. J. Moss,[146] J. Moss,[150,jj] K. Motohashi,[163] R. Mount,[150] E. Mountricha,[29] E. J. W. Moyse,[100] S. Muanza,[99] F. Mueller,[113] J. Mueller,[135] R. S. P. Mueller,[112] D. Muenstermann,[87] P. Mullen,[55] G. A. Mullier,[20] F. J. Munoz Sanchez,[98] P. Murin,[28b] W. J. Murray,[176,141] A. Murrone,[66a,66b] M. Muškinja,[89] C. Mwewa,[32a] A. G. Myagkov,[140,kk] J. Myers,[127] M. Myska,[138] B. P. Nachman,[18] O. Nackenhorst,[45] K. Nagai,[131] R. Nagai,[79,ee] K. Nagano,[79] Y. Nagasaka,[60] K. Nagata,[167] M. Nagel,[50] E. Nagy,[99] A. M. Nairz,[35] Y. Nakahama,[115] K. Nakamura,[79] T. Nakamura,[161] I. Nakano,[123] F. Napolitano,[59a] R. F. Naranjo Garcia,[44] R. Narayan,[11] D. I. Narrias Villar,[59a] I. Naryshkin,[134] T. Naumann,[44] G. Navarro,[22] R. Nayyar,[7] H. A. Neal,[103] P. Y. Nechaeva,[108] T. J. Neep,[142] A. Negri,[68a,68b] M. Negrini,[23b] S. Nektarijevic,[117] C. Nellist,[51] M. E. Nelson,[131] S. Nemecek,[137] P. Nemethy,[121] M. Nessi,[35,ll] M. S. Neubauer,[171] M. Neumann,[180] P. R. Newman,[21] T. Y. Ng,[61c] Y. S. Ng,[19] H. D. N. Nguyen,[99] T. Nguyen Manh,[107] E. Nibigira,[37] R. B. Nickerson,[131] R. Nicolaidou,[142] J. Nielsen,[143] N. Nikiforou,[11] V. Nikolaenko,[140,kk] I. Nikolic-Audit,[132] K. Nikolopoulos,[21] P. Nilsson,[29] Y. Ninomiya,[79] A. Nisati,[70a] N. Nishu,[58c] R. Nisius,[113] I. Nitsche,[45] T. Nitta,[177] T. Nobe,[161] Y. Noguchi,[83] M. Nomachi,[129] I. Nomidis,[33] M. A. Nomura,[29] T. Nooney,[90] M. Nordberg,[35] N. Norjoharuddeen,[131] T. Novak,[89] O. Novgorodova,[46] R. Novotny,[138] M. Nozaki,[79] L. Nozka,[126] K. Ntekas,[169] E. Nurse,[92] F. Nuti,[102] F. G. Oakham,[33,d] H. Oberlack,[113] T. Obermann,[24] J. Ocariz,[132] A. Ochi,[80] I. Ochoa,[38] J. P. Ochoa-Ricoux,[144a] K. O'Connor,[26] S. Oda,[85] S. Odaka,[79] A. Oh,[98] S. H. Oh,[47] C. C. Ohm,[151] H. Ohman,[170] H. Oide,[53b,53a] H. Okawa,[167] Y. Okazaki,[83] Y. Okumura,[161] T. Okuyama,[79] A. Olariu,[27b] L. F. Oleiro Seabra,[136a] S. A. Olivares Pino,[144a] D. Oliveira Damazio,[29] J. L. Oliver,[1] M. J. R. Olsson,[36] A. Olszewski,[82] J. Olszowska,[82] D. C. O'Neil,[149] A. Onofre,[136a,136e] K. Onogi,[115] P. U. E. Onyisi,[11] H. Oppen,[130] M. J. Oreglia,[36] Y. Oren,[159] D. Orestano,[72a,72b] E. C. Orgill,[98] N. Orlando,[61b] A. A. O'Rourke,[44] R. S. Orr,[165] B. Osculati,[53b,53a,a] V. O'Shea,[55] R. Ospanov,[58a] G. Otero y Garzon,[30] H. Otono,[85] M. Ouchrif,[34d] F. Ould-Saada,[130] A. Ouraou,[142] Q. Ouyang,[15a] M. Owen,[55] R. E. Owen,[21] V. E. Ozcan,[12c] N. Ozturk,[8] K. Pachal,[149] A. Pacheco Pages,[14] L. Pacheco Rodriguez,[142] C. Padilla Aranda,[14] S. Pagan Griso,[18] M. Paganini,[181] G. Palacino,[63] S. Palazzo,[40b,40a] S. Palestini,[35] M. Palka,[81b] D. Pallin,[37] I. Panagoulias,[10] C. E. Pandini,[52] J. G. Panduro Vazquez,[91] P. Pani,[35] L. Paolozzi,[52] T. D. Papadopoulou,[10] K. Papageorgiou,[9,s] A. Paramonov,[6] D. Paredes Hernandez,[61b] B. Parida,[58c] A. J. Parker,[87] K. A. Parker,[44] M. A. Parker,[31] F. Parodi,[53b,53a] J. A. Parsons,[38] U. Parzefall,[50] V. R. Pascuzzi,[165] J. M. P. Pasner,[143] E. Pasqualucci,[70a] S. Passaggio,[53b] F. Pastore,[91] P. Pasuwan,[43a,43b] S. Pataraia,[97] J. R. Pater,[98] A. Pathak,[179,e] T. Pauly,[35] B. Pearson,[113] M. Pedersen,[130] S. Pedraza Lopez,[172] R. Pedro,[136a,136b] S. V. Peleganchuk,[120b,120a] O. Penc,[137] C. Peng,[15d] H. Peng,[58a] J. Penwell,[63] B. S. Peralva,[78a] M. M. Perego,[142] A. P. Pereira Peixoto,[136a] D. V. Perepelitsa,[29] F. Peri,[19] L. Perini,[66a,66b] H. Pernegger,[35] S. Perrella,[67a,67b]

V. D. Peshekhonov,[77,a] K. Peters,[44] R. F. Y. Peters,[98] B. A. Petersen,[35] T. C. Petersen,[39] E. Petit,[56] A. Petridis,[1] C. Petridou,[160] P. Petroff,[128] E. Petrolo,[70a] M. Petrov,[131] F. Petrucci,[72a,72b] N. E. Pettersson,[100] A. Peyaud,[142] R. Pezoa,[144b] T. Pham,[102] F. H. Phillips,[104] P. W. Phillips,[141] G. Piacquadio,[152] E. Pianori,[176] A. Picazio,[100] M. A. Pickering,[131] R. Piegaia,[30] J. E. Pilcher,[36] A. D. Pilkington,[98] M. Pinamonti,[71a,71b] J. L. Pinfold,[3] M. Pitt,[178] M-A. Pleier,[29] V. Pleskot,[139] E. Plotnikova,[77] D. Pluth,[76] P. Podberezko,[120b,120a] R. Poettgen,[94] R. Poggi,[68a,68b] L. Poggioli,[128] I. Pogrebnyak,[104] D. Pohl,[24] I. Pokharel,[51] G. Polesello,[68a] A. Poley,[44] A. Policicchio,[40b,40a] R. Polifka,[35] A. Polini,[23b] C. S. Pollard,[44] V. Polychronakos,[29] D. Ponomarenko,[110] L. Pontecorvo,[70a] G. A. Popeneciu,[27d] D. M. Portillo Quintero,[132] S. Pospisil,[138] K. Potamianos,[44] I. N. Potrap,[77] C. J. Potter,[31] H. Potti,[11] T. Poulsen,[94] J. Poveda,[35] M. E. Pozo Astigarraga,[35] P. Pralavorio,[99] S. Prell,[76] D. Price,[98] M. Primavera,[65a] S. Prince,[101] N. Proklova,[110] K. Prokofiev,[61c] F. Prokoshin,[144b] S. Protopopescu,[29] J. Proudfoot,[6] M. Przybycien,[81a] A. Puri,[171] P. Puzo,[128] J. Qian,[103] Y. Qin,[98] A. Quadt,[51] M. Queitsch-Maitland,[44] A. Qureshi,[1] S. K. Radhakrishnan,[152] P. Rados,[102] F. Ragusa,[66a,66b] G. Rahal,[95] J. A. Raine,[98] S. Rajagopalan,[29] T. Rashid,[128] S. Raspopov,[5] M. G. Ratti,[66a,66b] D. M. Rauch,[44] F. Rauscher,[112] S. Rave,[97] B. Ravina,[146] I. Ravinovich,[178] J. H. Rawling,[98] M. Raymond,[35] A. L. Read,[130] N. P. Readioff,[56] M. Reale,[65a,65b] D. M. Rebuzzi,[68a,68b] A. Redelbach,[175] G. Redlinger,[29] R. Reece,[143] R. G. Reed,[32c] K. Reeves,[42] L. Rehnisch,[19] J. Reichert,[133] A. Reiss,[97] C. Rembser,[35] H. Ren,[15d] M. Rescigno,[70a] S. Resconi,[66a] E. D. Resseguie,[133] S. Rettie,[173] E. Reynolds,[21] O. L. Rezanova,[120b,120a] P. Reznicek,[139] R. Richter,[113] S. Richter,[92] E. Richter-Was,[81b] O. Ricken,[24] M. Ridel,[132] P. Rieck,[113] C. J. Riegel,[180] O. Rifki,[44] M. Rijssenbeek,[152] A. Rimoldi,[68a,68b] M. Rimoldi,[20] L. Rinaldi,[23b] G. Ripellino,[151] B. Ristić,[35] E. Ritsch,[35] I. Riu,[14] J. C. Rivera Vergara,[144a] F. Rizatdinova,[125] E. Rizvi,[90] C. Rizzi,[14] R. T. Roberts,[98] S. H. Robertson,[101,m] A. Robichaud-Veronneau,[101] D. Robinson,[31] J. E. M. Robinson,[44] A. Robson,[55] E. Rocco,[97] C. Roda,[69a,69b] Y. Rodina,[99,mm] S. Rodriguez Bosca,[172] A. Rodriguez Perez,[14] D. Rodriguez Rodriguez,[172] A. M. Rodríguez Vera,[166b] S. Roe,[35] C. S. Rogan,[57] O. Røhne,[130] R. Röhrig,[113] C. P. A. Roland,[63] J. Roloff,[57] A. Romaniouk,[110] M. Romano,[23b,23a] E. Romero Adam,[172] N. Rompotis,[88] M. Ronzani,[121] L. Roos,[132] S. Rosati,[70a] K. Rosbach,[50] P. Rose,[143] N-A. Rosien,[51] E. Rossi,[67a,67b] L. P. Rossi,[53b] L. Rossini,[66a,66b] J. H. N. Rosten,[31] R. Rosten,[145] M. Rotaru,[27b] J. Rothberg,[145] D. Rousseau,[128] D. Roy,[32c] A. Rozanov,[99] Y. Rozen,[158] X. Ruan,[32c] F. Rubbo,[150] F. Rühr,[50] A. Ruiz-Martinez,[33] Z. Rurikova,[50] N. A. Rusakovich,[77] H. L. Russell,[101] J. P. Rutherfoord,[7] N. Ruthmann,[35] E. M. Rüttinger,[44,nn] Y. F. Ryabov,[134] M. Rybar,[171] G. Rybkin,[128] S. Ryu,[6] A. Ryzhov,[140] G. F. Rzehorz,[51] P. Sabatini,[51] G. Sabato,[118] S. Sacerdoti,[128] H. F-W. Sadrozinski,[143] R. Sadykov,[77] F. Safai Tehrani,[70a] P. Saha,[119] M. Sahinsoy,[59a] M. Saimpert,[44] M. Saito,[161] T. Saito,[161] H. Sakamoto,[161] A. Sakharov,[121,ff] D. Salamani,[52] G. Salamanna,[72a,72b] J. E. Salazar Loyola,[144b] D. Salek,[118] P. H. Sales De Bruin,[170] D. Salihagic,[113] A. Salnikov,[150] J. Salt,[172] D. Salvatore,[40b,40a] F. Salvatore,[153] A. Salvucci,[61a,61b,61c] A. Salzburger,[35] D. Sammel,[50] D. Sampsonidis,[160] D. Sampsonidou,[160] J. Sánchez,[172] A. Sanchez Pineda,[64a,64c] H. Sandaker,[130] C. O. Sander,[44] M. Sandhoff,[180] C. Sandoval,[22] D. P. C. Sankey,[141] M. Sannino,[53b,53a] Y. Sano,[115] A. Sansoni,[49] C. Santoni,[37] H. Santos,[136a] I. Santoyo Castillo,[153] A. Sapronov,[77] J. G. Saraiva,[136a,136d] O. Sasaki,[79] K. Sato,[167] E. Sauvan,[5] P. Savard,[165,d] N. Savic,[113] R. Sawada,[161] C. Sawyer,[141] L. Sawyer,[93,u] C. Sbarra,[23b] A. Sbrizzi,[23b,23a] T. Scanlon,[92] D. A. Scannicchio,[169] J. Schaarschmidt,[145] P. Schacht,[113] B. M. Schachtner,[112] D. Schaefer,[36] L. Schaefer,[133] J. Schaeffer,[97] S. Schaepe,[35] U. Schäfer,[97] A. C. Schaffer,[128] D. Schaile,[112] R. D. Schamberger,[152] N. Scharmberg,[98] V. A. Schegelsky,[134] D. Scheirich,[139] F. Schenck,[19] M. Schernau,[169] C. Schiavi,[53b,53a] S. Schier,[143] L. K. Schildgen,[24] Z. M. Schillaci,[26] E. J. Schioppa,[35] M. Schioppa,[40b,40a] K. E. Schleicher,[50] S. Schlenker,[35] K. R. Schmidt-Sommerfeld,[113] K. Schmieden,[35] C. Schmitt,[97] S. Schmitt,[44] S. Schmitz,[97] U. Schnoor,[50] L. Schoeffel,[142] A. Schoening,[59b] E. Schopf,[24] M. Schott,[97] J. F. P. Schouwenberg,[117] J. Schovancova,[35] S. Schramm,[52] N. Schuh,[97] A. Schulte,[97] H-C. Schultz-Coulon,[59a] M. Schumacher,[50] B. A. Schumm,[143] Ph. Schune,[142] A. Schwartzman,[150] T. A. Schwarz,[103] H. Schweiger,[98] Ph. Schwemling,[142] R. Schwienhorst,[104] A. Sciandra,[24] G. Sciolla,[26] M. Scornajenghi,[40b,40a] F. Scuri,[69a] F. Scutti,[102] L. M. Scyboz,[113] J. Searcy,[103] C. D. Sebastiani,[70a,70b] P. Seema,[24] S. C. Seidel,[116] A. Seiden,[143] J. M. Seixas,[78b] G. Sekhniaidze,[67a] K. Sekhon,[103] S. J. Sekula,[41] N. Semprini-Cesari,[23b,23a] S. Senkin,[37] C. Serfon,[130] L. Serin,[128] L. Serkin,[64a,64b] M. Sessa,[72a,72b] H. Severini,[124] F. Sforza,[168] A. Sfyrla,[52] E. Shabalina,[51] J. D. Shahinian,[143] N. W. Shaikh,[43a,43b] L. Y. Shan,[15a] R. Shang,[171] J. T. Shank,[25] M. Shapiro,[18] A. S. Sharma,[1] A. Sharma,[131] P. B. Shatalov,[109] K. Shaw,[64a,64b] S. M. Shaw,[98] A. Shcherbakova,[134] C. Y. Shehu,[153] Y. Shen,[124] N. Sherafati,[33] A. D. Sherman,[25] P. Sherwood,[92] L. Shi,[155,oo] S. Shimizu,[80] C. O. Shimmin,[181] M. Shimojima,[114] I. P. J. Shipsey,[131] S. Shirabe,[85] M. Shiyakova,[77] J. Shlomi,[178] A. Shmeleva,[108] D. Shoaleh Saadi,[107] M. J. Shochet,[36] S. Shojaii,[102] D. R. Shope,[124] S. Shrestha,[122] E. Shulga,[110] P. Sicho,[137] A. M. Sickles,[171] P. E. Sidebo,[151] E. Sideras Haddad,[32c] O. Sidiropoulou,[175] A. Sidoti,[23b,23a] F. Siegert,[46] Dj. Sijacki,[16] J. Silva,[136a] M. Silva Jr.,[179]

S. B. Silverstein,[43a] L. Simic,[77] S. Simion,[128] E. Simioni,[97] B. Simmons,[92] M. Simon,[97] P. Sinervo,[165] N. B. Sinev,[127] M. Sioli,[23b,23a] G. Siragusa,[175] I. Siral,[103] S. Yu. Sivoklokov,[111] J. Sjölin,[43a,43b] M. B. Skinner,[87] P. Skubic,[124] M. Slater,[21] T. Slavicek,[138] M. Slawinska,[82] K. Sliwa,[168] R. Slovak,[139] V. Smakhtin,[178] B. H. Smart,[5] J. Smiesko,[28a] N. Smirnov,[110] S. Yu. Smirnov,[110] Y. Smirnov,[110] L. N. Smirnova,[111] O. Smirnova,[94] J. W. Smith,[51] M. N. K. Smith,[38] R. W. Smith,[38] M. Smizanska,[87] K. Smolek,[138] A. A. Snesarev,[108] I. M. Snyder,[127] S. Snyder,[29] R. Sobie,[174,m] F. Socher,[46] A. M. Soffa,[169] A. Soffer,[159] A. Søgaard,[48] D. A. Soh,[155] G. Sokhrannyi,[89] C. A. Solans Sanchez,[35] M. Solar,[138] E. Yu. Soldatov,[110] U. Soldevila,[172] A. A. Solodkov,[140] A. Soloshenko,[77] O. V. Solovyanov,[140] V. Solovyev,[134] P. Sommer,[146] H. Son,[168] W. Song,[141] A. Sopczak,[138] F. Sopkova,[28b] D. Sosa,[59b] C. L. Sotiropoulou,[69a,69b] S. Sottocornola,[68a,68b] R. Soualah,[64a,64c,pp] A. M. Soukharev,[120b,120a] D. South,[44] B. C. Sowden,[91] S. Spagnolo,[65a,65b] M. Spalla,[113] M. Spangenberg,[176] F. Spanò,[91] D. Sperlich,[19] F. Spettel,[113] T. M. Spieker,[59a] R. Spighi,[23b] G. Spigo,[35] L. A. Spiller,[102] M. Spousta,[139] A. Stabile,[66a,66b] R. Stamen,[59a] S. Stamm,[19] E. Stanecka,[82] R. W. Stanek,[6] C. Stanescu,[72a] M. M. Stanitzki,[44] B. Stapf,[118] S. Stapnes,[130] E. A. Starchenko,[140] G. H. Stark,[36] J. Stark,[56] S. H Stark,[39] P. Staroba,[137] P. Starovoitov,[59a] S. Stärz,[35] R. Staszewski,[82] M. Stegler,[44] P. Steinberg,[29] B. Stelzer,[149] H. J. Stelzer,[35] O. Stelzer-Chilton,[166a] H. Stenzel,[54] T. J. Stevenson,[90] G. A. Stewart,[55] M. C. Stockton,[127] G. Stoicea,[27b] P. Stolte,[51] S. Stonjek,[113] A. Straessner,[46] J. Strandberg,[151] S. Strandberg,[43a,43b] M. Strauss,[124] P. Strizenec,[28b] R. Ströhmer,[175] D. M. Strom,[127] R. Stroynowski,[41] A. Strubig,[48] S. A. Stucci,[29] B. Stugu,[17] J. Stupak,[124] N. A. Styles,[44] D. Su,[150] J. Su,[135] S. Suchek,[59a] Y. Sugaya,[129] M. Suk,[138] V. V. Sulin,[108] D. M. S. Sultan,[52] S. Sultansoy,[4c] T. Sumida,[83] S. Sun,[103] X. Sun,[3] K. Suruliz,[153] C. J. E. Suster,[154] M. R. Sutton,[153] S. Suzuki,[79] M. Svatos,[137] M. Swiatlowski,[36] S. P. Swift,[2] A. Sydorenko,[97] I. Sykora,[28a] T. Sykora,[139] D. Ta,[97] K. Tackmann,[44,qq] J. Taenzer,[159] A. Taffard,[169] R. Tafirout,[166a] E. Tahirovic,[90] N. Taiblum,[159] H. Takai,[29] R. Takashima,[84] E. H. Takasugi,[113] K. Takeda,[80] T. Takeshita,[147] Y. Takubo,[79] M. Talby,[99] A. A. Talyshev,[120b,120a] J. Tanaka,[161] M. Tanaka,[163] R. Tanaka,[128] W. Tang,[47] R. Tanioka,[80] B. B. Tannenwald,[122] S. Tapia Araya,[144b] S. Tapprogge,[97] A. Tarek Abouelfadl Mohamed,[132] S. Tarem,[158] G. Tarna,[27b,p] G. F. Tartarelli,[66a] P. Tas,[139] M. Tasevsky,[137] T. Tashiro,[83] E. Tassi,[40b,40a] A. Tavares Delgado,[136a,136b] Y. Tayalati,[34e] A. C. Taylor,[116] A. J. Taylor,[48] G. N. Taylor,[102] P. T. E. Taylor,[102] W. Taylor,[166b] A. S. Tee,[87] P. Teixeira-Dias,[91] D. Temple,[149] H. Ten Kate,[35] P. K. Teng,[155] J. J. Teoh,[129] F. Tepel,[180] S. Terada,[79] K. Terashi,[161] J. Terron,[96] S. Terzo,[14] M. Testa,[49] R. J. Teuscher,[165,m] S. J. Thais,[181] T. Theveneaux-Pelzer,[44] F. Thiele,[39] J. P. Thomas,[21] A. S. Thompson,[55] P. D. Thompson,[21] L. A. Thomsen,[181] E. Thomson,[133] Y. Tian,[38] R. E. Ticse Torres,[51] V. O. Tikhomirov,[108,rr] Yu. A. Tikhonov,[120b,120a] S. Timoshenko,[110] P. Tipton,[181] S. Tisserant,[99] K. Todome,[163] S. Todorova-Nova,[5] S. Todt,[46] J. Tojo,[85] S. Tokár,[28a] K. Tokushuku,[79] E. Tolley,[122] M. Tomoto,[115] L. Tompkins,[150] K. Toms,[116] B. Tong,[57] P. Tornambe,[50] E. Torrence,[127] H. Torres,[46] E. Torró Pastor,[145] C. Tosciri,[131] J. Toth,[99,ss] F. Touchard,[99] D. R. Tovey,[146] C. J. Treado,[121] T. Trefzger,[175] F. Tresoldi,[153] A. Tricoli,[29] I. M. Trigger,[166a] S. Trincaz-Duvoid,[132] M. F. Tripiana,[14] W. Trischuk,[165] B. Trocmé,[56] A. Trofymov,[44] C. Troncon,[66a] M. Trovatelli,[174] F. Trovato,[153] L. Truong,[32b] M. Trzebinski,[82] A. Trzupek,[82] F. Tsai,[44] K. W. Tsang,[61a] J. C-L. Tseng,[131] P. V. Tsiareshka,[105] N. Tsirintanis,[9] S. Tsiskaridze,[14] V. Tsiskaridze,[152] E. G. Tskhadadze,[157a] I. I. Tsukerman,[109] V. Tsulaia,[18] S. Tsuno,[79] D. Tsybychev,[152] Y. Tu,[61b] A. Tudorache,[27b] V. Tudorache,[27b] T. T. Tulbure,[27a] A. N. Tuna,[57] S. Turchikhin,[77] D. Turgeman,[178] I. Turk Cakir,[4b,tt] R. Turra,[66a] P. M. Tuts,[38] G. Ucchielli,[23b,23a] I. Ueda,[79] M. Ughetto,[43a,43b] F. Ukegawa,[167] G. Unal,[35] A. Undrus,[29] G. Unel,[169] F. C. Ungaro,[102] Y. Unno,[79] K. Uno,[161] J. Urban,[28b] P. Urquijo,[102] P. Urrejola,[97] G. Usai,[8] J. Usui,[79] L. Vacavant,[99] V. Vacek,[138] B. Vachon,[101] K. O. H. Vadla,[130] A. Vaidya,[92] C. Valderanis,[112] E. Valdes Santurio,[43a,43b] M. Valente,[52] S. Valentinetti,[23b,23a] A. Valero,[172] L. Valéry,[44] R. A. Vallance,[21] A. Vallier,[5] J. A. Valls Ferrer,[172] T. R. Van Daalen,[14] W. Van Den Wollenberg,[118] H. Van der Graaf,[118] P. Van Gemmeren,[6] J. Van Nieuwkoop,[149] I. Van Vulpen,[118] M. C. van Woerden,[118] M. Vanadia,[71a,71b] W. Vandelli,[35] A. Vaniachine,[164] P. Vankov,[118] R. Vari,[70a] E. W. Varnes,[7] C. Varni,[53b,53a] T. Varol,[41] D. Varouchas,[128] A. Vartapetian,[8] K. E. Varvell,[154] G. A. Vasquez,[144b] J. G. Vasquez,[181] F. Vazeille,[37] D. Vazquez Furelos,[14] T. Vazquez Schroeder,[101] J. Veatch,[51] V. Vecchio,[72a,72b] L. M. Veloce,[165] F. Veloso,[136a,136c] S. Veneziano,[70a] A. Ventura,[65a,65b] M. Venturi,[174] N. Venturi,[35] V. Vercesi,[68a] M. Verducci,[72a,72b] W. Verkerke,[118] A. T. Vermeulen,[118] J. C. Vermeulen,[118] M. C. Vetterli,[149,d] N. Viaux Maira,[144b] O. Viazlo,[94] I. Vichou,[171,a] T. Vickey,[146] O. E. Vickey Boeriu,[146] G. H. A. Viehhauser,[131] S. Viel,[18] L. Vigani,[131] M. Villa,[23b,23a] M. Villaplana Perez,[66a,66b] E. Vilucchi,[49] M. G. Vincter,[33] V. B. Vinogradov,[77] A. Vishwakarma,[44] C. Vittori,[23b,23a] I. Vivarelli,[153] S. Vlachos,[10] M. Vogel,[180] P. Vokac,[138] G. Volpi,[14] S. E. Von Buddenbrock,[32c] E. Von Toerne,[24] V. Vorobel,[139] K. Vorobev,[110] M. Vos,[172] J. H. Vossebeld,[88] N. Vranjes,[16] M. Vranjes Milosavljevic,[16] V. Vrba,[138] M. Vreeswijk,[118] T. Šfiligoj,[89] R. Vuillermet,[35] I. Vukotic,[36] T. Ženiš,[28a]

L. Živković,[16] P. Wagner,[24] W. Wagner,[180] J. Wagner-Kuhr,[112] H. Wahlberg,[86] S. Wahrmund,[46] K. Wakamiya,[80] J. Walder,[87] R. Walker,[112] W. Walkowiak,[148] V. Wallangen,[43a,43b] A. M. Wang,[57] C. Wang,[58b,p] F. Wang,[179] H. Wang,[18] H. Wang,[3] J. Wang,[154] J. Wang,[59b] P. Wang,[41] Q. Wang,[124] R.-J. Wang,[132] R. Wang,[58a] R. Wang,[6] S. M. Wang,[155] T. Wang,[38] W. Wang,[155,uu] W. X. Wang,[58a,vv] Y. Wang,[58a] Z. Wang,[58c] C. Wanotayaroj,[44] A. Warburton,[101] C. P. Ward,[31] D. R. Wardrope,[92] A. Washbrook,[48] P. M. Watkins,[21] A. T. Watson,[21] M. F. Watson,[21] G. Watts,[145] S. Watts,[98] B. M. Waugh,[92] A. F. Webb,[11] S. Webb,[97] C. Weber,[181] M. S. Weber,[20] S. A. Weber,[33] S. M. Weber,[59a] J. S. Webster,[6] A. R. Weidberg,[131] B. Weinert,[63] J. Weingarten,[51] M. Weirich,[97] C. Weiser,[50] P. S. Wells,[35] T. Wenaus,[29] T. Wengler,[35] S. Wenig,[35] N. Wermes,[24] M. D. Werner,[76] P. Werner,[35] M. Wessels,[59a] T. D. Weston,[20] K. Whalen,[127] N. L. Whallon,[145] A. M. Wharton,[87] A. S. White,[103] A. White,[8] M. J. White,[1] R. White,[144b] D. Whiteson,[169] B. W. Whitmore,[87] F. J. Wickens,[141] W. Wiedenmann,[179] M. Wielers,[141] C. Wiglesworth,[39] L. A. M. Wiik-Fuchs,[50] A. Wildauer,[113] F. Wilk,[98] H. G. Wilkens,[35] H. H. Williams,[133] S. Williams,[31] C. Willis,[104] S. Willocq,[100] J. A. Wilson,[21] I. Wingerter-Seez,[5] E. Winkels,[153] F. Winklmeier,[127] O. J. Winston,[153] B. T. Winter,[24] M. Wittgen,[150] M. Wobisch,[93] A. Wolf,[97] T. M. H. Wolf,[118] R. Wolff,[99] M. W. Wolter,[82] H. Wolters,[136a,136c] V. W. S. Wong,[173] N. L. Woods,[143] S. D. Worm,[21] B. K. Wosiek,[82] K. W. Woźniak,[82] K. Wraight,[55] M. Wu,[36] S. L. Wu,[179] X. Wu,[52] Y. Wu,[58a] T. R. Wyatt,[98] B. M. Wynne,[48] S. Xella,[39] Z. Xi,[103] L. Xia,[15b] D. Xu,[15a] H. Xu,[58a] L. Xu,[29] T. Xu,[142] W. Xu,[103] B. Yabsley,[154] S. Yacoob,[32a] K. Yajima,[129] D. P. Yallup,[92] D. Yamaguchi,[163] Y. Yamaguchi,[163] A. Yamamoto,[79] T. Yamanaka,[161] F. Yamane,[80] M. Yamatani,[161] T. Yamazaki,[161] Y. Yamazaki,[80] Z. Yan,[25] H. J. Yang,[58c,58d] H. T. Yang,[18] S. Yang,[75] Y. Yang,[161] Y. Yang,[155] Z. Yang,[17] W-M. Yao,[18] Y. C. Yap,[44] Y. Yasu,[79] E. Yatsenko,[5] K. H. Yau Wong,[24] J. Ye,[41] S. Ye,[29] I. Yeletskikh,[77] E. Yigitbasi,[25] E. Yildirim,[97] K. Yorita,[177] K. Yoshihara,[133] C. J. S. Young,[35] C. Young,[150] J. Yu,[8] J. Yu,[76] X. Yue,[59a] S. P. Y. Yuen,[24] I. Yusuff,[31,ww] B. Zabinski,[82] G. Zacharis,[10] R. Zaidan,[14] A. M. Zaitsev,[140,kk] N. Zakharchuk,[44] J. Zalieckas,[17] S. Zambito,[57] D. Zanzi,[35] C. Zeitnitz,[180] G. Zemaityte,[131] J. C. Zeng,[171] Q. Zeng,[150] O. Zenin,[140] D. Zerwas,[128] M. Zgubič,[131] D. F. Zhang,[58b] D. Zhang,[103] F. Zhang,[179] G. Zhang,[58a,vv] H. Zhang,[15c] J. Zhang,[6] L. Zhang,[50] L. Zhang,[58a] M. Zhang,[171] P. Zhang,[15c] R. Zhang,[58a,p] R. Zhang,[24] X. Zhang,[58b] Y. Zhang,[15d] Z. Zhang,[128] X. Zhao,[41] Y. Zhao,[58b,128,x] Z. Zhao,[58a] A. Zhemchugov,[77] B. Zhou,[103] C. Zhou,[179] L. Zhou,[41] M. S. Zhou,[15d] M. Zhou,[152] N. Zhou,[58c] Y. Zhou,[7] C. G. Zhu,[58b] H. L. Zhu,[58a] H. Zhu,[15a] J. Zhu,[103] Y. Zhu,[58a] X. Zhuang,[15a] K. Zhukov,[108] V. Zhulanov,[120b,120a] A. Zibell,[175] D. Zieminska,[63] N. I. Zimine,[77] S. Zimmermann,[50] Z. Zinonos,[113] M. Zinser,[97] M. Ziolkowski,[148] G. Zobernig,[179] A. Zoccoli,[23b,23a] K. Zoch,[51] T. G. Zorbas,[146] R. Zou,[36] M. Zur Nedden,[19] and L. Zwalinski[35]

(ATLAS Collaboration)

[1]*Department of Physics, University of Adelaide, Adelaide, Australia*
[2]*Physics Department, SUNY Albany, Albany, New York, USA*
[3]*Department of Physics, University of Alberta, Edmonton, Alberta, Canada*
[4a]*Department of Physics, Ankara University, Ankara, Turkey*
[4b]*Istanbul Aydin University, Istanbul, Turkey*
[4c]*Division of Physics, TOBB University of Economics and Technology, Ankara, Turkey*
[5]*LAPP, Université Grenoble Alpes, Université Savoie Mont Blanc, CNRS/IN2P3, Annecy, France*
[6]*High Energy Physics Division, Argonne National Laboratory, Argonne, Illinois, USA*
[7]*Department of Physics, University of Arizona, Tucson, Arizona, USA*
[8]*Department of Physics, University of Texas at Arlington, Arlington, Texas, USA*
[9]*Physics Department, National and Kapodistrian University of Athens, Athens, Greece*
[10]*Physics Department, National Technical University of Athens, Zografou, Greece*
[11]*Department of Physics, University of Texas at Austin, Austin, Texas, USA*
[12a]*Bahcesehir University, Faculty of Engineering and Natural Sciences, Istanbul, Turkey*
[12b]*Istanbul Bilgi University, Faculty of Engineering and Natural Sciences, Istanbul, Turkey*
[12c]*Department of Physics, Bogazici University, Istanbul, Turkey*
[12d]*Department of Physics Engineering, Gaziantep University, Gaziantep, Turkey*
[13]*Institute of Physics, Azerbaijan Academy of Sciences, Baku, Azerbaijan*
[14]*Institut de Física d'Altes Energies (IFAE), Barcelona Institute of Science and Technology, Barcelona, Spain*
[15a]*Institute of High Energy Physics, Chinese Academy of Sciences, Beijing, China*
[15b]*Physics Department, Tsinghua University, Beijing, China*
[15c]*Department of Physics, Nanjing University, Nanjing, China*

[15d]University of Chinese Academy of Science (UCAS), Beijing, China
[16]Institute of Physics, University of Belgrade, Belgrade, Serbia
[17]Department for Physics and Technology, University of Bergen, Bergen, Norway
[18]Physics Division, Lawrence Berkeley National Laboratory and University of California, Berkeley, California, USA
[19]Institut für Physik, Humboldt Universität zu Berlin, Berlin, Germany
[20]Albert Einstein Center for Fundamental Physics and Laboratory for High Energy Physics, University of Bern, Bern, Switzerland
[21]School of Physics and Astronomy, University of Birmingham, Birmingham, United Kingdom
[22]Centro de Investigaciónes, Universidad Antonio Nariño, Bogota, Colombia
[23a]Dipartimento di Fisica e Astronomia, Università di Bologna, Bologna, Italy
[23b]INFN Sezione di Bologna, Italy
[24]Physikalisches Institut, Universität Bonn, Bonn, Germany
[25]Department of Physics, Boston University, Boston, Massachusetts, USA
[26]Department of Physics, Brandeis University, Waltham, Massachusetts, USA
[27a]Transilvania University of Brasov, Brasov, Romania
[27b]Horia Hulubei National Institute of Physics and Nuclear Engineering, Bucharest, Romania
[27c]Department of Physics, Alexandru Ioan Cuza University of Iasi, Iasi, Romania
[27d]National Institute for Research and Development of Isotopic and Molecular Technologies, Physics Department, Cluj-Napoca, Romania
[27e]University Politehnica Bucharest, Bucharest, Romania
[27f]West University in Timisoara, Timisoara, Romania
[28a]Faculty of Mathematics, Physics and Informatics, Comenius University, Bratislava, Slovak Republic
[28b]Department of Subnuclear Physics, Institute of Experimental Physics of the Slovak Academy of Sciences, Kosice, Slovak Republic
[29]Physics Department, Brookhaven National Laboratory, Upton, New York, USA
[30]Departamento de Física, Universidad de Buenos Aires, Buenos Aires, Argentina
[31]Cavendish Laboratory, University of Cambridge, Cambridge, United Kingdom
[32a]Department of Physics, University of Cape Town, Cape Town, South Africa
[32b]Department of Mechanical Engineering Science, University of Johannesburg, Johannesburg, South Africa
[32c]School of Physics, University of the Witwatersrand, Johannesburg, South Africa
[33]Department of Physics, Carleton University, Ottawa, Ontario, Canada
[34a]Faculté des Sciences Ain Chock, Réseau Universitaire de Physique des Hautes Energies-Université Hassan II, Casablanca, Morocco
[34b]Centre National de l'Energie des Sciences Techniques Nucleaires (CNESTEN), Rabat, Morocco
[34c]Faculté des Sciences Semlalia, Université Cadi Ayyad, LPHEA-Marrakech, Morocco
[34d]Faculté des Sciences, Université Mohamed Premier and LPTPM, Oujda, Morocco
[34e]Faculté des sciences, Université Mohammed V, Rabat, Morocco
[35]CERN, Geneva, Switzerland
[36]Enrico Fermi Institute, University of Chicago, Chicago, Illinois, USA
[37]LPC, Université Clermont Auvergne, CNRS/IN2P3, Clermont-Ferrand, France
[38]Nevis Laboratory, Columbia University, Irvington, New York, USA
[39]Niels Bohr Institute, University of Copenhagen, Copenhagen, Denmark
[40a]Dipartimento di Fisica, Università della Calabria, Rende, Italy
[40b]INFN Gruppo Collegato di Cosenza, Laboratori Nazionali di Frascati, Italy
[41]Physics Department, Southern Methodist University, Dallas, Texas, USA
[42]Physics Department, University of Texas at Dallas, Richardson, Texas, USA
[43a]Department of Physics, Stockholm University, Sweden
[43b]Oskar Klein Centre, Stockholm, Sweden
[44]Deutsches Elektronen-Synchrotron DESY, Hamburg and Zeuthen, Germany
[45]Lehrstuhl für Experimentelle Physik IV, Technische Universität Dortmund, Dortmund, Germany
[46]Institut für Kern- und Teilchenphysik, Technische Universität Dresden, Dresden, Germany
[47]Department of Physics, Duke University, Durham, North Carolina, USA
[48]SUPA - School of Physics and Astronomy, University of Edinburgh, Edinburgh, United Kingdom
[49]INFN e Laboratori Nazionali di Frascati, Frascati, Italy
[50]Physikalisches Institut, Albert-Ludwigs-Universität Freiburg, Freiburg, Germany
[51]II. Physikalisches Institut, Georg-August-Universität Göttingen, Göttingen, Germany
[52]Département de Physique Nucléaire et Corpusculaire, Université de Genève, Genève, Switzerland
[53a]Dipartimento di Fisica, Università di Genova, Genova, Italy

[53b]*INFN Sezione di Genova, Italy*
[54]*II. Physikalisches Institut, Justus-Liebig-Universität Giessen, Giessen, Germany*
[55]*SUPA - School of Physics and Astronomy, University of Glasgow, Glasgow, United Kingdom*
[56]*LPSC, Université Grenoble Alpes, CNRS/IN2P3, Grenoble INP, Grenoble, France*
[57]*Laboratory for Particle Physics and Cosmology, Harvard University, Cambridge, Massachusetts, USA*
[58a]*Department of Modern Physics and State Key Laboratory of Particle Detection and Electronics, University of Science and Technology of China, Hefei, China*
[58b]*Institute of Frontier and Interdisciplinary Science and Key Laboratory of Particle Physics and Particle Irradiation (MOE), Shandong University, Qingdao, China*
[58c]*School of Physics and Astronomy, Shanghai Jiao Tong University, KLPPAC-MoE, SKLPPC, Shanghai, China*
[58d]*Tsung-Dao Lee Institute, Shanghai, China*
[59a]*Kirchhoff-Institut für Physik, Ruprecht-Karls-Universität Heidelberg, Heidelberg, Germany*
[59b]*Physikalisches Institut, Ruprecht-Karls-Universität Heidelberg, Heidelberg, Germany*
[60]*Faculty of Applied Information Science, Hiroshima Institute of Technology, Hiroshima, Japan*
[61a]*Department of Physics, Chinese University of Hong Kong, Shatin, N.T., Hong Kong, China*
[61b]*Department of Physics, University of Hong Kong, Hong Kong, China*
[61c]*Department of Physics and Institute for Advanced Study, Hong Kong University of Science and Technology, Clear Water Bay, Kowloon, Hong Kong, China*
[62]*Department of Physics, National Tsing Hua University, Hsinchu, Taiwan*
[63]*Department of Physics, Indiana University, Bloomington, Indiana, USA*
[64a]*INFN Gruppo Collegato di Udine, Sezione di Trieste, Udine, Italy*
[64b]*ICTP, Trieste, Italy*
[64c]*Dipartimento di Chimica, Fisica e Ambiente, Università di Udine, Udine, Italy*
[65a]*INFN Sezione di Lecce, Italy*
[65b]*Dipartimento di Matematica e Fisica, Università del Salento, Lecce, Italy*
[66a]*INFN Sezione di Milano, Italy*
[66b]*Dipartimento di Fisica, Università di Milano, Milano, Italy*
[67a]*INFN Sezione di Napoli, Italy*
[67b]*Dipartimento di Fisica, Università di Napoli, Napoli, Italy*
[68a]*INFN Sezione di Pavia, Italy*
[68b]*Dipartimento di Fisica, Università di Pavia, Pavia, Italy*
[69a]*INFN Sezione di Pisa, Italy*
[69b]*Dipartimento di Fisica E. Fermi, Università di Pisa, Pisa, Italy*
[70a]*INFN Sezione di Roma, Italy*
[70b]*Dipartimento di Fisica, Sapienza Università di Roma, Roma, Italy*
[71a]*INFN Sezione di Roma Tor Vergata, Italy*
[71b]*Dipartimento di Fisica, Università di Roma Tor Vergata, Roma, Italy*
[72a]*INFN Sezione di Roma Tre, Italy*
[72b]*Dipartimento di Matematica e Fisica, Università Roma Tre, Roma, Italy*
[73a]*INFN-TIFPA, Italy*
[73b]*Università degli Studi di Trento, Trento, Italy*
[74]*Institut für Astro- und Teilchenphysik, Leopold-Franzens-Universität, Innsbruck, Austria*
[75]*University of Iowa, Iowa City, Iowa, USA*
[76]*Department of Physics and Astronomy, Iowa State University, Ames, Iowa, USA*
[77]*Joint Institute for Nuclear Research, Dubna, Russia*
[78a]*Departamento de Engenharia Elétrica, Universidade Federal de Juiz de Fora (UFJF), Juiz de Fora, Brazil*
[78b]*Universidade Federal do Rio De Janeiro COPPE/EE/IF, Rio de Janeiro, Brazil*
[78c]*Universidade Federal de São João del Rei (UFSJ), São João del Rei, Brazil*
[78d]*Instituto de Física, Universidade de São Paulo, São Paulo, Brazil*
[79]*KEK, High Energy Accelerator Research Organization, Tsukuba, Japan*
[80]*Graduate School of Science, Kobe University, Kobe, Japan*
[81a]*AGH University of Science and Technology, Faculty of Physics and Applied Computer Science, Krakow, Poland*
[81b]*Marian Smoluchowski Institute of Physics, Jagiellonian University, Krakow, Poland*
[82]*Institute of Nuclear Physics Polish Academy of Sciences, Krakow, Poland*
[83]*Faculty of Science, Kyoto University, Kyoto, Japan*
[84]*Kyoto University of Education, Kyoto, Japan*

[85]Research Center for Advanced Particle Physics and Department of Physics, Kyushu University, Fukuoka, Japan
[86]Instituto de Física La Plata, Universidad Nacional de La Plata and CONICET, La Plata, Argentina
[87]Physics Department, Lancaster University, Lancaster, United Kingdom
[88]Oliver Lodge Laboratory, University of Liverpool, Liverpool, United Kingdom
[89]Department of Experimental Particle Physics, Jožef Stefan Institute and Department of Physics, University of Ljubljana, Ljubljana, Slovenia
[90]School of Physics and Astronomy, Queen Mary University of London, London, United Kingdom
[91]Department of Physics, Royal Holloway University of London, Egham, United Kingdom
[92]Department of Physics and Astronomy, University College London, London, United Kingdom
[93]Louisiana Tech University, Ruston, Louisiana, USA
[94]Fysiska institutionen, Lunds universitet, Lund, Sweden
[95]Centre de Calcul de l'Institut National de Physique Nucléaire et de Physique des Particules (IN2P3), Villeurbanne, France
[96]Departamento de Física Teorica C-15 and CIAFF, Universidad Autónoma de Madrid, Madrid, Spain
[97]Institut für Physik, Universität Mainz, Mainz, Germany
[98]School of Physics and Astronomy, University of Manchester, Manchester, United Kingdom
[99]CPPM, Aix-Marseille Université, CNRS/IN2P3, Marseille, France
[100]Department of Physics, University of Massachusetts, Amherst, Massachusetts, USA
[101]Department of Physics, McGill University, Montreal, Quebec, Canada
[102]School of Physics, University of Melbourne, Victoria, Australia
[103]Department of Physics, University of Michigan, Ann Arbor, Michigan, USA
[104]Department of Physics and Astronomy, Michigan State University, East Lansing, Michigan, USA
[105]B.I. Stepanov Institute of Physics, National Academy of Sciences of Belarus, Minsk, Belarus
[106]Research Institute for Nuclear Problems of Byelorussian State University, Minsk, Belarus
[107]Group of Particle Physics, University of Montreal, Montreal, Quebec, Canada
[108]P.N. Lebedev Physical Institute of the Russian Academy of Sciences, Moscow, Russia
[109]Institute for Theoretical and Experimental Physics (ITEP), Moscow, Russia
[110]National Research Nuclear University MEPhI, Moscow, Russia
[111]D.V. Skobeltsyn Institute of Nuclear Physics, M.V. Lomonosov Moscow State University, Moscow, Russia
[112]Fakultät für Physik, Ludwig-Maximilians-Universität München, München, Germany
[113]Max-Planck-Institut für Physik (Werner-Heisenberg-Institut), München, Germany
[114]Nagasaki Institute of Applied Science, Nagasaki, Japan
[115]Graduate School of Science and Kobayashi-Maskawa Institute, Nagoya University, Nagoya, Japan
[116]Department of Physics and Astronomy, University of New Mexico, Albuquerque, New Mexico, USA
[117]Institute for Mathematics, Astrophysics and Particle Physics, Radboud University Nijmegen/Nikhef, Nijmegen, Netherlands
[118]Nikhef National Institute for Subatomic Physics and University of Amsterdam, Amsterdam, Netherlands
[119]Department of Physics, Northern Illinois University, DeKalb, Illinois, USA
[120a]Budker Institute of Nuclear Physics, SB RAS, Novosibirsk, Russia
[120b]Novosibirsk State University Novosibirsk, Russia
[121]Department of Physics, New York University, New York, New York, USA
[122]Ohio State University, Columbus, Ohio, USA
[123]Faculty of Science, Okayama University, Okayama, Japan
[124]Homer L. Dodge Department of Physics and Astronomy, University of Oklahoma, Norman, Oklahoma, USA
[125]Department of Physics, Oklahoma State University, Stillwater, Oklahoma, USA
[126]Palacký University, RCPTM, Joint Laboratory of Optics, Olomouc, Czech Republic
[127]Center for High Energy Physics, University of Oregon, Eugene, Oregon, USA
[128]LAL, Université Paris-Sud, CNRS/IN2P3, Université Paris-Saclay, Orsay, France
[129]Graduate School of Science, Osaka University, Osaka, Japan
[130]Department of Physics, University of Oslo, Oslo, Norway
[131]Department of Physics, Oxford University, Oxford, United Kingdom
[132]LPNHE, Sorbonne Université, Paris Diderot Sorbonne Paris Cité, CNRS/IN2P3, Paris, France
[133]Department of Physics, University of Pennsylvania, Philadelphia, Pennsylvania, USA
[134]Konstantinov Nuclear Physics Institute of National Research Centre "Kurchatov Institute", PNPI, St. Petersburg, Russia
[135]Department of Physics and Astronomy, University of Pittsburgh, Pittsburgh, Pennsylvania, USA
[136a]Laboratório de Instrumentação e Física Experimental de Partículas-LIP, Portugal

[136b]*Departamento de Física, Faculdade de Ciências, Universidade de Lisboa, Lisboa, Portugal*
[136c]*Departamento de Física, Universidade de Coimbra, Coimbra, Portugal*
[136d]*Centro de Física Nuclear da Universidade de Lisboa, Lisboa, Portugal*
[136e]*Departamento de Física, Universidade do Minho, Braga, Portugal*
[136f]*Departamento de Física Teorica y del Cosmos, Universidad de Granada, Granada (Spain), Spain*
[136g]*Dep Física and CEFITEC of Faculdade de Ciências e Tecnologia, Universidade Nova de Lisboa, Caparica, Portugal*
[137]*Institute of Physics, Academy of Sciences of the Czech Republic, Prague, Czech Republic*
[138]*Czech Technical University in Prague, Prague, Czech Republic*
[139]*Charles University, Faculty of Mathematics and Physics, Prague, Czech Republic*
[140]*State Research Center Institute for High Energy Physics, NRC KI, Protvino, Russia*
[141]*Particle Physics Department, Rutherford Appleton Laboratory, Didcot, United Kingdom*
[142]*IRFU, CEA, Université Paris-Saclay, Gif-sur-Yvette, France*
[143]*Santa Cruz Institute for Particle Physics, University of California Santa Cruz, Santa Cruz, California, USA*
[144a]*Departamento de Física, Pontificia Universidad Católica de Chile, Santiago, Chile*
[144b]*Departamento de Física, Universidad Técnica Federico Santa María, Valparaíso, Chile*
[145]*Department of Physics, University of Washington, Seattle, Washington, USA*
[146]*Department of Physics and Astronomy, University of Sheffield, Sheffield, United Kingdom*
[147]*Department of Physics, Shinshu University, Nagano, Japan*
[148]*Department Physik, Universität Siegen, Siegen, Germany*
[149]*Department of Physics, Simon Fraser University, Burnaby, British Columbia, Canada*
[150]*SLAC National Accelerator Laboratory, Stanford, California, USA*
[151]*Physics Department, Royal Institute of Technology, Stockholm, Sweden*
[152]*Departments of Physics and Astronomy, Stony Brook University, Stony Brook, New York, USA*
[153]*Department of Physics and Astronomy, University of Sussex, Brighton, United Kingdom*
[154]*School of Physics, University of Sydney, Sydney, Australia*
[155]*Institute of Physics, Academia Sinica, Taipei, Taiwan*
[156]*Academia Sinica Grid Computing, Institute of Physics, Academia Sinica, Taipei, Taiwan*
[157a]*E. Andronikashvili Institute of Physics, Iv. Javakhishvili Tbilisi State University, Tbilisi, Georgia*
[157b]*High Energy Physics Institute, Tbilisi State University, Tbilisi, Georgia*
[158]*Department of Physics, Technion, Israel Institute of Technology, Haifa, Israel*
[159]*Raymond and Beverly Sackler School of Physics and Astronomy, Tel Aviv University, Tel Aviv, Israel*
[160]*Department of Physics, Aristotle University of Thessaloniki, Thessaloniki, Greece*
[161]*International Center for Elementary Particle Physics and Department of Physics, University of Tokyo, Tokyo, Japan*
[162]*Graduate School of Science and Technology, Tokyo Metropolitan University, Tokyo, Japan*
[163]*Department of Physics, Tokyo Institute of Technology, Tokyo, Japan*
[164]*Tomsk State University, Tomsk, Russia*
[165]*Department of Physics, University of Toronto, Toronto, Ontario, Canada*
[166a]*TRIUMF, Vancouver, British Columbia, Canada*
[166b]*Department of Physics and Astronomy, York University, Toronto, Ontario, Canada*
[167]*Division of Physics and Tomonaga Center for the History of the Universe, Faculty of Pure and Applied Sciences, University of Tsukuba, Tsukuba, Japan*
[168]*Department of Physics and Astronomy, Tufts University, Medford, Massachusetts, USA*
[169]*Department of Physics and Astronomy, University of California Irvine, Irvine, California, USA*
[170]*Department of Physics and Astronomy, University of Uppsala, Uppsala, Sweden*
[171]*Department of Physics, University of Illinois, Urbana, Illinois, USA*
[172]*Instituto de Física Corpuscular (IFIC), Centro Mixto Universidad de Valencia-CSIC, Valencia, Spain*
[173]*Department of Physics, University of British Columbia, Vancouver, British Columbia, Canada*
[174]*Department of Physics and Astronomy, University of Victoria, Victoria, British Columbia, Canada*
[175]*Fakultät für Physik und Astronomie, Julius-Maximilians-Universität Würzburg, Würzburg, Germany*
[176]*Department of Physics, University of Warwick, Coventry, United Kingdom*
[177]*Waseda University, Tokyo, Japan*
[178]*Department of Particle Physics, Weizmann Institute of Science, Rehovot, Israel*
[179]*Department of Physics, University of Wisconsin, Madison, Wisconsin, USA*
[180]*Fakultät für Mathematik und Naturwissenschaften, Fachgruppe Physik, Bergische Universität Wuppertal, Wuppertal, Germany*
[181]*Department of Physics, Yale University, New Haven, Connecticut, USA*
[182]*Yerevan Physics Institute, Yerevan, Armenia*

[a]Deceased.
[b]Also at Department of Physics, King's College London, London, United Kingdom.
[c]Also at Institute of Physics, Azerbaijan Academy of Sciences, Baku, Azerbaijan.
[d]Also at TRIUMF, Vancouver, British Columbia, Canada.
[e]Also at Department of Physics and Astronomy, University of Louisville, Louisville, Kentucky, USA.
[f]Also at Department of Physics, California State University, Fresno, California, USA.
[g]Also at Department of Physics, University of Fribourg, Fribourg, Switzerland.
[h]Also at II. Physikalisches Institut, Georg-August-Universität Göttingen, Göttingen, Germany.
[i]Also at Departament de Fisica de la Universitat Autonoma de Barcelona, Barcelona, Spain.
[j]Also at Tomsk State University, Tomsk, and Moscow Institute of Physics and Technology State University, Dolgoprudny, Russia.
[k]Also at The Collaborative Innovation Center of Quantum Matter (CICQM), Beijing, China.
[l]Also at Universita di Napoli Parthenope, Napoli, Italy.
[m]Also at Institute of Particle Physics (IPP), Canada.
[n]Also at Dipartimento di Fisica E. Fermi, Università di Pisa, Pisa, Italy.
[o]Also at Horia Hulubei National Institute of Physics and Nuclear Engineering, Bucharest, Romania.
[p]Also at CPPM, Aix-Marseille Université, CNRS/IN2P3, Marseille, France.
[q]Also at Department of Physics, St. Petersburg State Polytechnical University, St. Petersburg, Russia.
[r]Also at Borough of Manhattan Community College, City University of New York, New York, USA.
[s]Also at Department of Financial and Management Engineering, University of the Aegean, Chios, Greece.
[t]Also at Centre for High Performance Computing, CSIR Campus, Rosebank, Cape Town, South Africa.
[u]Also at Louisiana Tech University, Ruston, Louisiana, USA.
[v]Also at Institucio Catalana de Recerca i Estudis Avancats, ICREA, Barcelona, Spain.
[w]Also at Department of Physics, University of Michigan, Ann Arbor, Michigan, USA.
[x]Also at LAL, Université Paris-Sud, CNRS/IN2P3, Université Paris-Saclay, Orsay, France.
[y]Also at Graduate School of Science, Osaka University, Osaka, Japan.
[z]Also at Physikalisches Institut, Albert-Ludwigs-Universität Freiburg, Freiburg, Germany.
[aa]Also at Institute for Mathematics, Astrophysics and Particle Physics, Radboud University Nijmegen/Nikhef, Nijmegen, Netherlands.
[bb]Also at Near East University, Nicosia, North Cyprus, Mersin, Turkey.
[cc]Also at Institute of Theoretical Physics, Ilia State University, Tbilisi, Georgia.
[dd]Also at CERN, Geneva, Switzerland.
[ee]Also at Ochadai Academic Production, Ochanomizu University, Tokyo, Japan.
[ff]Also at Manhattan College, New York, New York, USA.
[gg]Also at Hellenic Open University, Patras, Greece.
[hh]Also at The City College of New York, New York, New York, USA.
[ii]Also at Departamento de Física Teorica y del Cosmos, Universidad de Granada, Granada (Spain), Spain.
[jj]Also at Department of Physics, California State University, Sacramento, California, USA.
[kk]Also at Moscow Institute of Physics and Technology State University, Dolgoprudny, Russia.
[ll]Also at Département de Physique Nucléaire et Corpusculaire, Université de Genève, Genève, Switzerland.
[mm]Also at Institut de Física d'Altes Energies (IFAE), Barcelona Institute of Science and Technology, Barcelona, Spain.
[nn]Also at Department of Physics and Astronomy, University of Sheffield, Sheffield, United Kingdom.
[oo]Also at School of Physics, Sun Yat-sen University, Guangzhou, China.
[pp]Also at Department of Applied Physics and Astronomy, University of Sharjah, Sharjah, United Arab Emirates.
[qq]Also at Institut für Experimentalphysik, Universität Hamburg, Hamburg, Germany.
[rr]Also at National Research Nuclear University MEPhI, Moscow, Russia.
[ss]Also at Institute for Particle and Nuclear Physics, Wigner Research Centre for Physics, Budapest, Hungary.
[tt]Also at Giresun University, Faculty of Engineering, Giresun, Turkey.
[uu]Also at Department of Physics, Nanjing University, Nanjing, China.
[vv]Also at Institute of Physics, Academia Sinica, Taipei, Taiwan.
[ww]Also at Department of Physics, University of Malaya, Kuala Lumpur, Malaysia.